leukemia. About 30% of AML patients have loss of expression of the ETV6/TEL protein;[47,48] mutations of *ETV6/TEL* were found in 2% of AML samples, and these mutants behaved in a dominant-negative fashion.[45] Interestingly, previous array-comparative genome hybridization analysis of normal karyotype AML showed duplication of 8q24.13-q24.21 (including the *MYC* gene) and deletion of 12p12.3 (including the *ETV6* gene);[55] this constellation of alterations was also observed in our study.

Our microarray analysis showed that regions with copy-number loss or gain of chromosomal material

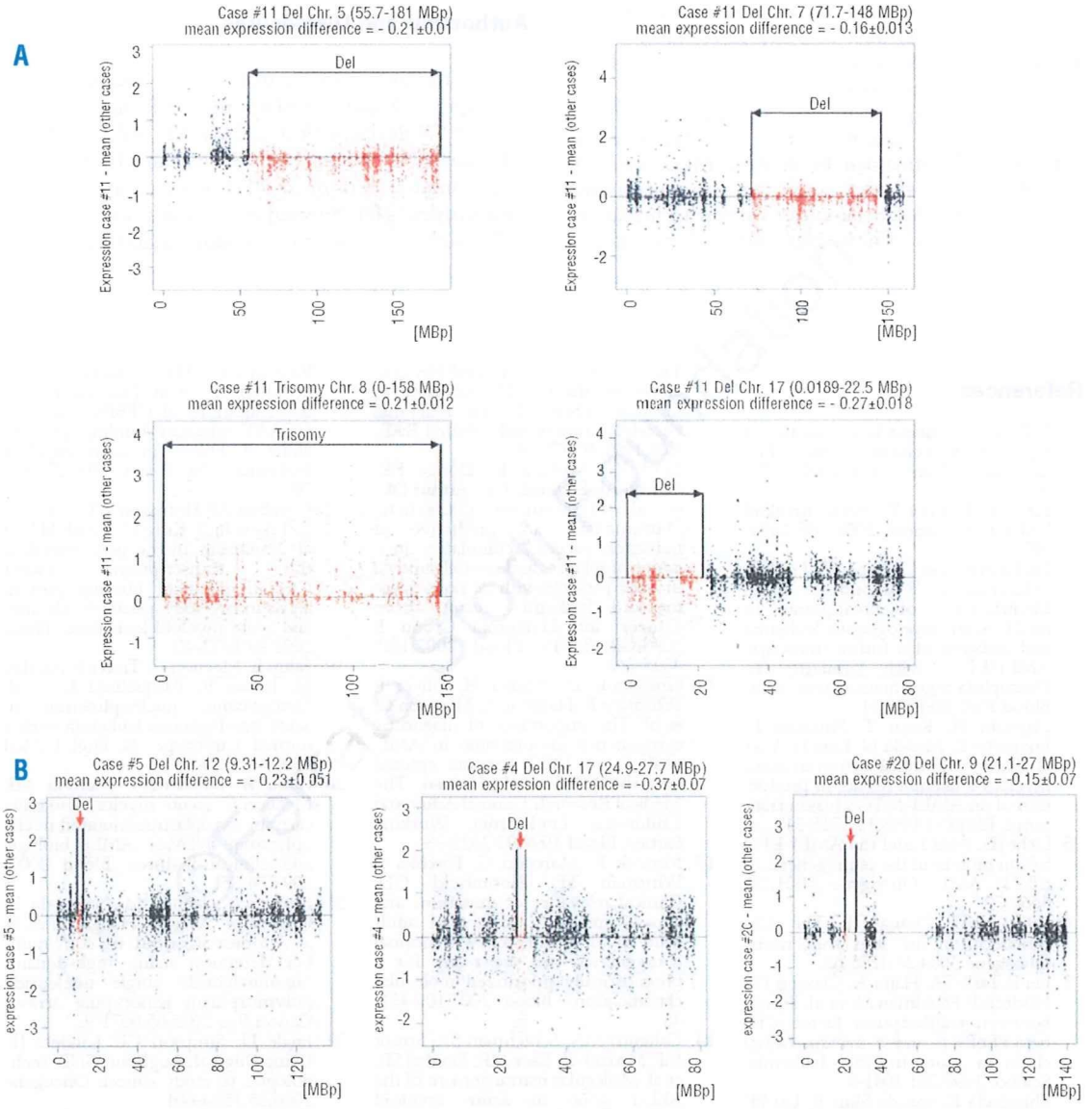

Figure 4. mRNA microarray analyses of acute myeloid leukemia samples. (**A**) Relationship between genomic abnormality and gene expression in acute myeloid leukemia case #11. mRNA microarray analysis was performed on all samples, and expression levels of acute myeloid leukemia cells from case #11 were compared to those of 37 normal karyotype acute myeloid leukemia samples. Affymetrix microarray analysis showed decreased average gene expression in the deleted regions, and increased average gene expression for trisomy 8: the difference of mean expression of genes located in the deleted region of chromosomes 5 (upper, left), 7 (upper, right), 17 (lower, right) and trisomy 8 (lower, left) were -0.21±0.01, -0.16±0.013, -0.27±0.018, and +0.21±0.012 (mean difference ± standard error), respectively. (**B**) Expression levels in acute myeloid leukemia cells from cases #20, #4 and #5 were compared with those in 36 normal karyotype AML samples. The differences in mean expression of genes located on the deleted region of chromosome 9 in case #20 (right), chromosome 17 in case #4 (middle), and chromosome 12 in case #5 (left) were -0.15±0.07, -0.37±0.07, and -0.23±0.051 (mean difference ± standard error), respectively. Each spot (black and red, Y-axis) indicates one gene and reflects the difference between each case and the mean of the other cases. Red spots represent genes located on an aberrant chromosome. The X-axis shows the chromosomal location.

were associated with either decreased or increased mRNA expression of genes in that same region, respectively, demonstrating the relationship between chromosomal status and gene expression. From an analysis perspective, we applied a descriptive approach and intended to assess plausibility of data. Some genes do indeed have higher expression values in deleted regions (Figure 4A, red points above zero) than in other cases, and some genes have lower values in trisomy (Figure 4A, red points below zero) than in other cases. However on average, expression in deleted regions is clearly lower than in non-deleted cases.

Because most regions are not recurring, we compared only one sample versus the rest (i.e. case #11 was compared with 37 normal karyotype AML/MDS cases; and cases #20, #4 and #5 were compared with other normal karyotype AML/MDS samples.) Various technical and biological sources of noise can confound the analysis. Overall, expression data appear to be consistent with chromosomal deletions and amplifications of the investigated regions. Further studies in larger cohorts of patients should enable prognostic stratification of patients in relation to their genomic changes and reveal new therapeutic targets.

Authorship and Disclosures

TA performed research, analyzed the data and wrote the paper; SO and MS performed SNP-chip analyses; GY and YN developed the CNAG; NK, AY, CWM and MD assisted in data analyses; SS, CH and TH provided AML samples, performed FISH analysis and aided in data analyses; HPK directed the overall study.

The authors declare no competing financial interests.

References

1. Kelly LM, Gilliland DG. Genetics of myeloid leukemias. Annu Rev Genomics Hum Genet 2002;3:179-98.
2. Estey E, Dohner H. Acute myeloid leukaemia. Lancet 2006;368:1894-907.
3. Erickson P, Gao J, Chang KS, Look T, Whisenant E, Raimondi S, et al. Identification of breakpoints in t(8;21) acute myelogenous leukemia and isolation of a fusion transcript, AML1/ETO, with similarity to Drosophila segmentation gene, runt. Blood 1992;80:1825-31.
4. Miyoshi H, Kozu T, Shimizu K, Enomoto K, Maseki N, Kaneko Y, et al. The t(8;21) translocation in acute myeloid leukemia results in production of an AML1-MTG8 fusion transcript. EMBO J 1993;12:2715-21.
5. Licht JD. AML1 and the AML1-ETO fusion protein in the pathogenesis of t(8;21) AML. Oncogene 2001;20:5660-79.
6. Peterson LF, Zhang DE. The 8;21 translocation in leukemogenesis. Oncogene 2004;23:4255-62.
7. Liu P, Tarlé SA, Hajra A, Claxton DF, Marlton P, Freedman M, et al. Fusion between transcription factor CBF beta/PEBP2 β and a myosin heavy chain in acute myeloid leukemia. Science 1993;261:1041-4.
8. Shigesada K, van de Sluis B, Liu PP. Mechanism of leukemogenesis by the inv(16) chimeric gene CBFB/PEBP2B-MHY11. Oncogene 2004;23:4297-307.
9. de Thé H, Chomienne C, Lanotte M, Degos L, Dejean A. The t(15;17) translocation of acute promyelocytic leukaemia fuses the retinoic acid receptor alpha gene to a novel transcribed locus. Nature 1990;347:558-61.
10. de Thé H, Lavau C, Marchio A, Chomienne C, Degos L, Dejean A. The PML-RAR-α fusion mRNA generated by the t(15;17) translocation in acute promyelocytic leukemia encodes a functionally altered RAR. Cell 1991;66:675-84.
11. Byrd JC, Mrózek K, Dodge RK, Carroll AJ, Edwards CG, Arthur DC, et al. Pretreatment cytogenetic abnormalities are predictive of induction success, cumulative incidence of relapse, and overall survival in adult patients with de novo acute myeloid leukemia: results from Cancer and Leukemia Group B (CALGB 8461). Blood 2002;100:4325-36.
12. Grimwade D, Walker H, Oliver F, Wheatley K, Harrison C, Harrison G, et al. The importance of diagnostic cytogenetics on outcome in AML: analysis of 1,612 patients entered into the MRC AML 10 trial. The Medical Research Council Adult and Children's Leukaemia Working Parties. Blood 1998;92:2322-33.
13. Mrozek K, Marcucci G, Paschka P, Whitman SP, Bloomfield CD. Clinical relevance of mutations and gene-expression changes in adult acute myeloid leukemia with normal cytogenetics: are we ready for a prognostically prioritized molecular classification? Blood 2007;109:431-48.
14. Caligiuri MA, Schichman SA, Strout MP, Mrózek K, Baer MR, Frankel SR, et al. Molecular rearrangement of the ALL-1 gene in acute myeloid leukemia without cytogenetic evidence of 11q23 chromosomal translocations. Cancer Res 1994;54:370-3.
15. Gilliland DG, Griffin JD. The roles of FLT3 in hematopoiesis and leukemia. Blood 2002;100:1532-42.
16. Reuter CW, Morgan MA, Bergmann L. Targeting the Ras signaling pathway: a rational, mechanism-based treatment for hematologic malignancies? Blood 2000;96:1655-69.
17. Pabst T, Mueller BU, Zhang P, Radomska HS, Narravula S, Schnittger S, et al. Dominant-negative mutations of CEBPA, encoding CCAAT/enhancer binding protein-alpha (C/EBPα), in acute myeloid leukemia. Nat Genet 2001;27:263-70.
18. Gombart AF, Hofmann WK, Kawano S, Takeuchi S, Krug U, Kwok SH, et al. Mutations in the gene encoding the transcription factor CCAAT/enhancer binding protein alpha in myelodysplastic syndromes and acute myeloid leukemias. Blood 2002;99:1332-40.
19. Falini B, Mecucci C, Tiacci E, Alcalay M, Rosati R, Pasqualucci L, et al. Cytoplasmic nucleophosmin in acute myelogenous leukemia with a normal karyotype. N Engl J Med 2005;352:254-66.
20. Falini B, Nicoletti I, Martelli MF, Mecucci C. Acute myeloid leukemia carrying cytoplasmic/mutated nucleophosmin (NPMc+ AML): biologic and clinical features. Blood 2007;109:874-85.
21. Nannya Y, Sanada M, Nakazaki K, Hosoya N, Wang L, Hangaishi A, et al. A robust algorithm for copy number detection using high-density oligonucleotide single nucleotide polymorphism genotyping arrays. Cancer Res 2005;65:6071-9.
22. Engle LJ, Simpson CL, Landers JE. Using high-throughput SNP technologies to study cancer. Oncogene 2006;25:1594-601.
23. Yamamoto G, Nannya Y, Kato M, Sanada M, Levine RL, Kawamata N, et al. Highly sensitive method for genomewide detection of allelic composition in nonpaired, primary tumor specimens by use of affymetrix single-nucleotide-polymorphism genotyping microarrays. Am J Hum Genet 2007;81:114-26.
24. Pfeifer D, Pantic M, Skatulla I, Rawluk J, Kreutz C, Martens UM, et al. Genome-wide analysis of DNA copy number changes and LOH in

CLL using high-density SNP arrays. Blood 2007;109:1202-10.
25. Lehmann S, Ogawa S, Raynaud SD, Sanada M, Nannya Y, Ticchioni M, et al. Molecular allelokaryotyping of early stage untreated chronic lymphocytic leukemia. Cancer 2008; 112:1296-305.
26. Mullighan CG, Goorha S, Radtke I, Miller CB, Coustan-Smith E, Dalton JD, et al. Genome-wide analysis of genetic alterations in acute lymphoblastic leukaemia. Nature 2007; 446:758-64.
27. Kawamata N, Ogawa S, Zimmermann M, Kato M, Sanada M, Hemminki K, et al. Molecular allelokaryotyping of pediatric acute lymphoblastic leukemias by high resolution single nucleotide polymorphism oligonucleotide genomic microarray. Blood 2008;111:776-84.
28. Flotho C, Steinemann D, Mullighan CG, Neale G, Mayer K, Kratz CP, et al. Genome-wide single-nucleotide polymorphism analysis in juvenile myelomonocytic leukemia identifies uniparental disomy surrounding the NF1 locus in cases associated with neurofibromatosis but not in cases with mutant RAS or PTPN11. Oncogene 2007;26:5816-21.
29. Fitzgibbon J, Iqbal S, Davies A, O'shea D, Carlotti E, Chaplin T, et al. Genome-wide detection of recurring sites of uniparental disomy in follicular and transformed follicular lymphoma. Leukemia 2007;21:1514-20.
30. Walker BA, Leone PE, Jenner MW, Li C, Gonzalez D, Johnson DC, et al. Integration of global SNP-based mapping and expression arrays reveals key regions, mechanisms, and genes important in the pathogenesis of multiple myeloma. Blood 2006;108:1733-43.
31. Raghavan M, Lillington DM, Skoulakis S, Debernardi S, Chaplin T, Foot NJ, et al. Genome-wide single nucleotide polymorphism analysis reveals frequent partial uniparental disomy due to somatic recombination in acute myeloid leukemias. Cancer Res 2005;65:375-8.
32. Fitzgibbon J, Smith LL, Raghavan M, Smith ML, Debernardi S, Skoulakis S, et al. Association between acquired uniparental disomy and homozygous gene mutation in acute myeloid leukemias. Cancer Res 2005;65:9152-4.
33. Tyybäkinoja A, Elonen E, Piippo K, Porkka K, Knuutila S. Oligonucleotide array-CGH reveals cryptic gene copy number alterations in karyotypically normal acute myeloid leukemia. Leukemia 2007;21:571-4.
34. Kiyoi H, Naoe T, Yokota S, Nakao M, Minami S, Kuriyama K, et al. Internal tandem duplication of FLT3 associated with leukocytosis in acute promyelocytic leukemia: Leukemia Study Group of the Ministry of Health and Welfare (Kohseisho). Leukemia 1997;11: 1447-52.
35. Schnittger S, Schoch C, Dugas M, Kern W, Staib P, Wuchter C, et al. Analysis of FLT3 length mutations in 1003 patients with acute myeloid leukemia: correlation to cytogenetics, FAB subtype, and prognosis in the AMLCG study and usefulness as a marker for the detection of minimal residual disease. Blood 2002; 100:59-66.
36. Schnittger S, Schoch C, Kern W, Mecucci C, Tschulik C, Martelli MF, et al. Nucleophosmin gene mutations are predictors of favorable prognosis in acute myelogenous leukemia with a normal karyotype. Blood 2005;106:3733-9.
37. Dicker F, Haferlach C, Kern W, Haferlach T, Schnittger S. Trisomy 13 is strongly associated with AML1/RUNX1 mutations and increased FLT3 expression in acute myeloid leukemia. Blood 2007;110: 1308-16.
38. Yin D, Xie D, Hofmann WK, Miller CW, Black KL, Koeffler HP. Methylation, expression, and mutation analysis of the cell cycle control genes in human brain tumors. Oncogene 2002;21:8372-8.
39. Bolstad BM, Irizarry RA, Astrand M, Speed TP. A comparison of normalization methods for high density oligonucleotide array data based on variance and bias. Bioinformatics 2003;19:185-93.
40. Haferlach T, Kohlmann A, Schnittger S, Dugas M, Hiddemann W, Kern W, et al. A global approach to the diagnosis of leukemia using gene expression profiling. Blood 2005;106:1189-98.
41. Hemann MT, Bric A, Teruya-Feldstein J, Herbst A, Nilsson JA, Cordon-Cardo C, et al. Evasion of the p53 tumour surveillance network by tumour-derived MYC mutants. Nature 2005;436:807-11.
42. Dang CV, O'Donnell KA, Juopperi T. The great MYC escape in tumorigenesis. Cancer Cell 2005;8:177-8.
43. Baxter EJ, Scott LM, Campbell PJ, East C, Fourouclas N, Swanton S, et al. Acquired mutation of the tyrosine kinase JAK2 in human myeloproliferative disorders. Lancet 2005; 365:1054-61.
44. Lee JW, Kim YG, Soung YH, Han KJ, Kim SY, Rhim HS, et al. The JAK2 V617F mutation in de novo acute myelogenous leukemias. Oncogene 2006;25:1434-6.
45. Illmer T, Schaich M, Ehninger G, Thiede C; DSIL2003 AML study group. Tyrosine kinase mutations of JAK2 are rare events in AML but influence prognosis of patients with CBF-leukemias. Haematologica 2007; 92:137-8.
46. Side LE, Emanuel PD, Taylor B, Franklin J, Thompson P, Castleberry RP, et al. Mutations of the NF1 gene in children with juvenile myelomonocytic leukemia without clinical evidence of neurofibromatosis, type 1. Blood 1998;92:267-72.
47. Hernández JM, González MB, García JL, Ferro MT, Gutiérrez NC, Marynen P, et al. Two cases of myeloid disorders and a t(8;12)(q12;p13). Haematologica 2000;85: 31-4.
48. Barjesteh van Waalwijk van Doorn-Khosrovani S, Spensberger D, de Knegt Y, Tang M, Löwenberg B, Delwel R. Somatic heterozygous mutations in ETV6 (TEL) and frequent absence of ETV6 protein in acute myeloid leukemia. Oncogene 2005;24:4129-37.
49. R Development Core Team. R: A language and environment for statistical computing. R Foundation for Statistical Computing, Vienna, Austria. 2007; ISBN 3-900051-07-0.
50. Serrano E, Carnicer MJ, Orantes V, Estivill C, Lasa A, Brunet S, et al. Uniparental disomy may be associated with microsatellite instability in acute myeloid leukemia (AML) with a normal karyotype. Leuk Lymphoma 2008;49:1178-83.
51. Gupta M, Raghavan M, Gale RE, Chelala C, Allen C, Molloy G, et al. Novel regions of acquired uniparental disomy discovered in acute myeloid leukemia. Genes Chromosomes Cancer 2008;47:729-39.
52. Raghavan M, Smith LL, Lillington DM, Chaplin T, Kakkas I, Molloy G, et al. Segmental uniparental disomy is a commonly acquired genetic event in relapsed acute myeloid leukemia. Blood 2008;112:814-21.
53. Gorletta TA, Gasparini P, D'Elios MM, Trubia M, Pelicci PG, Di Fiore PP. Frequent loss of heterozygosity without loss of genetic material in acute myeloid leukemia with a normal karyotype. Genes Chromosomes Cancer 2005;44: 334-7.
54. Tyybäkinoja A, Elonen E, Vauhkonen H, Saarela J, Knuutila S. Single nucleotide polymorphism microarray analysis of karyotypically normal acute myeloid leukemia reveals frequent copy number neutral loss of heterozygosity. Haematologica 2008; 93:631-2.

ASBMT
American Society for Blood and Marrow Transplantation

Exploration of the Genetic Basis of GVHD by Genetic Association Studies

Seishi Ogawa,[1,2] Aiko Matsubara,[1,2] Makoto Onizuka,[3] Koichi Kashiwase,[4] Masashi Sanada,[1,2] Motohiro Kato,[1,2] Yasuhito Nannya,[2] Yoshiki Akatsuka,[5] Masahiro Satake,[4] Junko Takita,[1,2] Shigeru Chiba,[6] Hiroo Saji,[7] Etsuko Maruya,[7] Hidetoshi Inoko,[3] Yasuo Morishima,[5] Yoshihisa Kodera,[8] Sasazuki Takehiko[9] On behalf of the Japan Marrow Donation Program (JMDP)

INTRODUCTION

Graft-versus-host disease (GVHD), as well as graft-versus-leukemia effect (GVL), are essentially allo-immune reactions, which are induced by the engrafted donor T cells that recognize the host-derived allo-antigens presented on their targets (Figure 1). In HLA-matched transplantation, these antigens are called minor histocompatibility antigens (mHags), and are typically defined by the host single nucleotide polymorphisms (SNPs) that are not shared by the donor and therefore considered to be genetically mismatched between the donor and the recipient [1–3]. Thus, the development of both allo-reactions absolutely depends on the presence of 1 or more mismatched mHags, although these reactions could be further modified by other genetic as well as environmental factors, including, cytokine polymorphisms and GVHD prophylaxis. So, in view of better preventing GVHD and specifically targeting allo-immunity to the tumor component, central questions are what mHAgs are responsible for the development of GVHD or GVL and what genetic factors can influence the overall reactions, which are the plausible targets of genome-wide association studies (GWAS) [4-8].

To identify the genetic basis of GVHD, we conducted GWAS by genotyping more than 500,000 SNPs using Affymetrix GeneChip platforms [9,10] in donors and recipients from 1,598 unrelated transplants performed through the Japan Marrow Donor Program (JMDP). All transplants were matched for HLA-A, B, C, DRB1, and DQB1 by high-resolution DNA typing, while 1033 (63%) transplants were mismatched for HLA-DPB1. Six hundred fifty-six (41.7%) and 245 (14.9%) of transplants had developed grade II-IV and grade III-IV of acute GVHD (aGVHD), respectively. Overall SNP call rates exceeded 98% both in donors and in recipients. Unobserved HapMap PhaseII SNPs were rigorously imputed from the genotyped SNPs [11-13]. After excluding those disqualified SNPs showing <95% call rate, deviation from Hardy-Weinberg equilibrium, or <5% minor allele frequency, 1,276,699 SNPs were tested for association with development of aGVHD and chronic GVHD (cGVHD), relapse, and overall survival (OS), by calculating log-rank statistics for each SNP. Statistical thresholds for genome-wide *P* value of .05 were determined empirically by doing 1,000 permutations for each analysis. Association tests were performed with regard to the simple genotype of donor and recipient SNPs. Alternatively, to identify possible mHag loci, GWAS were performed based on the allele-mismatch defined for each SNP locus, rather than simple SNP genotypes in donors and recipients. In the latter setting, associations were tested within the subgroups that shared particular HLA-types based on HLA-restriction. Generally speaking, the sample size of ~1,600 transplants in the current study was relatively small compared to the size of typical GWAS studies, and it was further reduced in the subgroup analysis [8]. Thus, it was likely that we could find only those mHag loci that were restricted to major HLA alleles and whose allele-mismatch conferred strong genetic effects on the development of GvHD [14,15]. However, this did not necessarily preclude conducting the current study, because it was such mHags that are thought to be clinically relevant.

From the [1]Core Research for Evolutional Science and Technology, Japan Science and Technology Agency, Japan; [2]University of Tokyo, Tokyo, Japan; [3]Tokai University, Isehara, Japan; [4]Tokyo Metroporitan Red Cross Blood Center, Tokyo, Japan; [5]Aichi Cancer Center, Nagoya, Japan; [6]Tsukub University, Tsukub, Japan; [7]NPO HLA Laboratory, Kyoto, Japan; [8]Aichi Medical Universiry, Aichi, Japan; and [9]International Medical Center of Japan, Tokyo, Japan.

Financial disclosure: See Acknowledgments on page 41.

Correspondence and reprint requests: Seishi Ogawa, MD, PhD, University of Tokyo, 7-3-1 Hongo, Bunkyo-ku, Tokyo 113-8655, Japan (e-mail: sogawa-tky@umin.ac.jp).

1083-8791/09/151S-0001$36.00/0
doi:10.1016/j.bbmt.2008.11.020

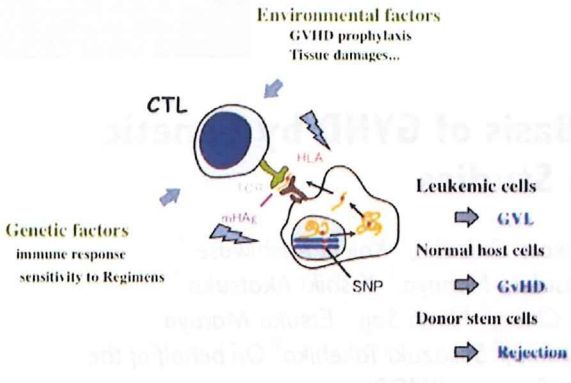

Figure 1. Allo-immunity plays central roles in HSCT.

In the analysis regarding genotype mismatch for aGVHD under the assumption of no HLA restriction, SNPs around the HLA-DPB1 locus showed strong association with the development of grade II-IV aGVHD with the maximum P value of 1.81×10^{-9} at rs6937034, and thus, the GWAS successfully captured the association of HLA-DPB1 allele mismatch as directly defined by high-resolution DNA typing (hazard ratio [HR] = 1.91, $P = 2.88 \times 10^{-13}$) (Figure 2) [16]. No other loci were identified that were significantly associated with aGVHD under the assumption of no HLA restrictions. To identify the target mHags for aGVHD, we further performed subgroup analyses, in which the analysis were confined to those transplants sharing major HLA types among the Japanese population [17]. Six loci were identified as candidate mHag loci. rs17473423 on chr12 was associated with the A*2402/B*5201/Cw*1201/DRB1*1501/DQB1*0601, which represents the most prevalent HLA haplotype among the Japanese population and shared in ~40% of unrelated transplants in Japanese (grade III-IV aGVHD, with maximum $P = 3.99 \times 10^{-13}$) (Figures 2b and 3b). rs9657655 on chr9 was associated with another common haplotype in Japanese, A*3303/B*4403/Cw*1403 (grade III-IV aGVHD with maximum $P = 8.56 \times 10^{-10}$) (Figures 2c and 3b). We found additional 4 loci that were associated with DQB1*0501, Cw*0102, B*5201, and Cw*1202. We also tested the association of GVHD with simple genotype in either recipients or donors, though which 2 recipient SNPs were found to be associated with aGVHD, rs5998746 on chr22 ($P = 3.41 \times 10^{-8}$) and rs11873016 on chr18 ($P = 1.26 \times 10^{-8}$), whereas no donor SNPs showed significant associations. Similarly, we identified 4 candidate SNPs associated with the development of severe cGVHD or relapse.

Our study provided a unique opportunity, in that a combination of 2 different genotypes, rather than mere genotypes in single individuals, is explored for association with particular disease phenotypes through whole genome association scanning. Although further replication studies and biologic confirmation are

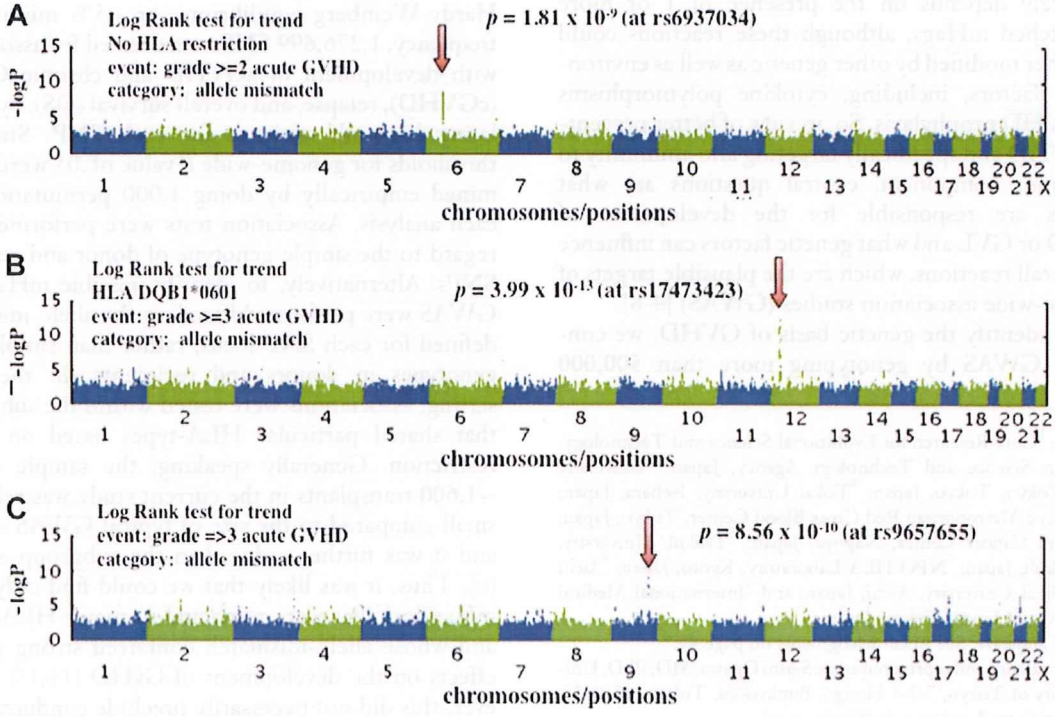

Figure 2. Representative results of GWAS based on genotype mismatch. $-\log_{10}P$ values are plotted in genetic order. Results are presented for association tests for genotype mismatch under no HLA restriction (A), and under the restriction to HLA DQB1*0601 (B) and HLA B*4403 (C).

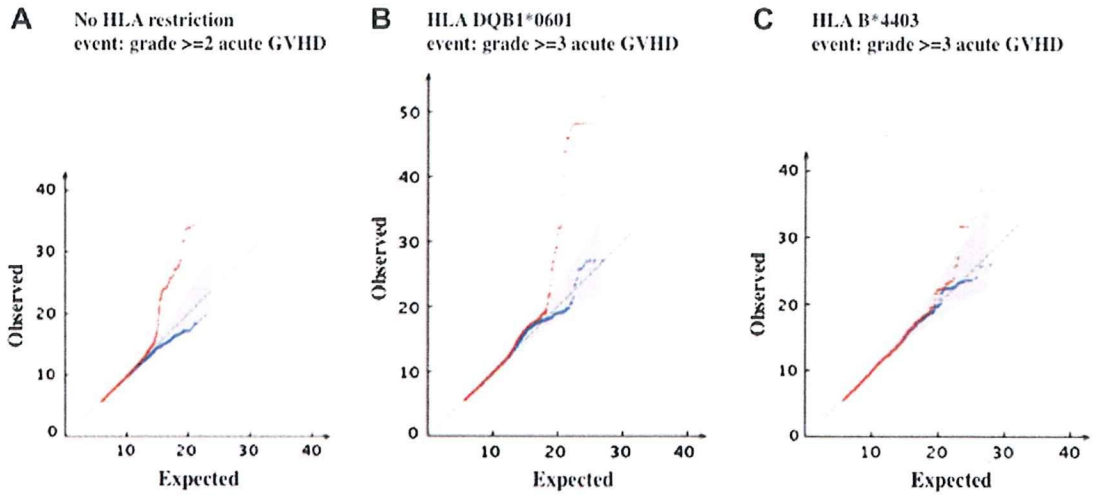

Figure 3. QQ-plots of the statistics. QQ-plots of the analysis of genotype mismatch under no restriction on HLA (A), and restriction to HLA DQB1*0601 (B) and HLA B*4403 (C) where observed test statistics values are plotted against expected values from 1000 random permutations (red); 95% confidence intervals are also provided by shadows. Only the plots for the top 20,000 results are presented. The QQ-plots excluding the SNPs that belong to the positive peak are also depicted in blue.

required, our results suggest that whole genome association studies of allo-SCT could provide a novel clue to our understanding of the genetic basis of GVHD.

ACKNOWLEDGMENTS

Financial disclosure: The authors have nothing to disclose.

REFERENCES

1. Bleakley M, Riddell SR. Molecules and mechanisms of the graft-versus-leukaemia effect. *Nat Rev Cancer*. 2004;4:371-380.
2. Shlomchik WD. Graft-versus-host disease. *Nat Rev Immunol*. 2007;7:340-352.
3. Brickner AG. Mechanisms of minor histocompatibility antigen immunogenicity: the role of infinitesimal versus structurally profound polymorphisms. *Immunol Res*. 2006;36:33-41.
4. Hirschhorn JN, Daly MJ. Genome-wide association studies for common diseases and complex traits. *Nat Rev Genet*. 2005;6: 95-108.
5. Kruglyak L. The road to genome-wide association studies. *Nat Rev Genet*. 2008;9:314-318.
6. McCarthy MI, Abecasis GR, Cardon LR, Goldstein DB, Little J, Ioannidis JP, Hirschhorn JN. Genome-wide association studies for complex traits: consensus, uncertainty and challenges. *Nat Rev Genet*. 2008;9:356-369.
7. Xavier RJ, Rioux JD. Genome-wide association studies: a new window into immune-mediated diseases. *Nat Rev Immunol*. 2008;8:631-643.
8. Topol EJ, Murray SS, Frazer KA. The genomics gold rush. *JAMA*. 2007;298:218-221.
9. Kennedy GC, Matsuzaki H, Dong S, et al. Large-scale genotyping of complex DNA. *Nat Biotechnol*. 2003;21:1233-1237.
10. Matsuzaki H, Dong S, Loi H, et al. Genotyping over 100,000 SNPs on a pair of oligonucleotide arrays. *Nat Methods*. 2004;1: 109-111.
11. Frazer KA, Ballinger DG, Cox DR, et al. A second generation human haplotype map of over 3.1 million SNPs. *Nature*. 2007; 449:851-861.
12. Marchini J, Howie B, Myers S, McVean G, Donnelly P. A new multipoint method for genome-wide association studies by imputation of genotypes. *Nat Genet*. 2007;39:906-913. 2007.
13. TheinternationlaHapMapconsortium. A haplotype map of the human genome. *Nature*. 2005;437:1299-1320.
14. Pe'er I, de Bakker PI, Maller J, Yelensky R, Altshuler D, Daly MJ. Evaluating and improving power in whole-genome association studies using fixed marker sets. *Nat Genet*. 2006;38: 663-667.
15. Nannya Y, Taura K, Kurokawa M, Chiba S, Ogawa S. Evaluation of genome-wide power of genetic association studies based on empirical data from the HapMap project. *Hum Mol Genet*. 2007;16:3494-3505.
16. Morishima Y, Yabe T, Matsuo K, et al. Effects of HLA allele and killer immunoglobulin-like receptor ligand matching on clinical outcome in leukemia patients undergoing transplantation with T-cell-replete marrow from an unrelated donor. *Biol Blood Marrow Transplant*. 2007;13:315-328.
17. Saito S, Ota S, Yamada E, Inoko H, Ota M. Allele frequencies and haplotypic associations defined by allelic DNA typing at HLA class I and class II loci in the Japanese population. *Tissue Antigens*. 2000;56:522-529.

Derivation of functional mature neutrophils from human embryonic stem cells

Yasuhisa Yokoyama,[1-3] Takahiro Suzuki,[1,2,4] Mamiko Sakata-Yanagimoto,[1-3] Keiki Kumano,[1,2] Katsumi Higashi,[5] Tsuyoshi Takato,[4] Mineo Kurokawa,[2] Seishi Ogawa,[1,4,6] and Shigeru Chiba[1,3]

[1]Department of Cell Therapy and Transplantation Medicine, University of Tokyo Hospital, Tokyo; [2]Department of Hematology and Oncology, Graduate School of Medicine, University of Tokyo, Tokyo; [3]Department of Clinical and Experimental Hematology, University of Tsukuba, Ibaraki; [4]Divison of Tissue Engineering, University of Tokyo Hospital, Tokyo; [5]Department of Clinical Hematology, School of Health Sciences, Kyorin University, Tokyo; and [6]The 21st Century COE Program, Graduate School of Medicine, University of Tokyo, Tokyo, Japan

Human embryonic stem cells (hESCs) proliferate infinitely and are pluripotent. Only a few reports, however, describe specific and efficient methods to induce hESCs to differentiate into mature blood cells. It is important to determine whether and how these cells, once generated, behave similarly with their in vivo–produced counterparts. We developed a method to induce hESCs to differentiate into mature neutrophils. Embryoid bodies were formed with bone morphogenic protein-4, stem cell factor (SCF), Flt-3 ligand (FL), interleukin-6 (IL-6)/IL-6 receptor fusion protein (FP6), and thrombopoietin (TPO). Cells derived from the embryoid bodies were cultured on a layer of irradiated OP9 cells with a combination of SCF, FL, FP6, IL-3, and TPO, which was later changed to granulocyte–colony-stimulating factor. Morphologically mature neutrophils were obtained in approximately 2 weeks with a purity and efficiency sufficient for functional analyses. The population of predominantly mature neutrophils (hESC-Neu's) showed superoxide production, phagocytosis, bactericidal activity, and chemotaxis similar to peripheral blood neutrophils from healthy subjects, although there were differences in the surface antigen expression patterns, such as decreased CD16 expression and aberrant CD64 and CD14 expression in hESC-Neu's. Thus, this is the first description of a detailed functional analysis of mature hESC-derived neutrophils. (Blood. 2009;113:6584-6592)

Introduction

Embryonic stem (ES) cells can self-renew and differentiate into cells derived from all 3 germ layers (ie, ectoderm, endoderm, and mesoderm). Both mouse and human ES cells give rise to mature blood cells of granulocyte/macrophage, erythroid, and megakaryoid lineages in vitro. For blood cell induction from ES cells, the majority of investigators use a coculturing system with mouse stromal cells such as S17[1] or OP9.[2,3] Embryoid body (EB) formation is also a commonly used method to obtain starting materials for further culture.[4-6] Cell surface antigens, such as CD45 and CD34, and colony-forming ability are used as blood cell markers. Hemangioblasts, which have the capacity to differentiate into both endothelial and blood cells, have also been produced.[7-9] Only a few studies, however, have achieved specific and effective induction of mature blood cells from ES cells, particularly human ES cells (hESCs).[10]

Human ESC-derived blood cells are potentially useful as a replacement for donation-based blood for transfusion in clinical settings, for drug discovery screening, and for monitoring drug efficacy and toxicity. The current blood donation system for transfusion is incapable of providing enough granulocytes for patients with life-threatening neutropenia, although granulocyte transfusion could have a potentially significant benefit for a certain population of severely neutropenic patients.[11,12] Given the large amount of neutrophils required for transfusion,[13] hESC-derived neutrophils might be a unique solution for this treatment demand. Therefore, the development of a highly effective method of neutrophil differentiation from hESCs is an important step for both clinical application of hESCs and granulocyte transfusion medicine.

The lack of an effective method for obtaining hESC-derived neutrophils with purity sufficient for functional analysis, however, has hampered progress in this field. Once neutrophils with a high purity can be generated from hESCs, it will be important to compare their activities with those of neutrophils produced in vivo, particularly given the fact that hESCs rarely give rise to hematopoietic stem cells in vitro,[14] and thus, that hESC-derived neutrophils might not be a progeny of hematopoietic stem cells. Here, we developed an effective method of deriving mature neutrophils from hESCs through EB formation and subsequent coculture with OP9, and analyzed their morphologic and phenotypic characteristics. We then performed functional analyses of hESC-derived neutrophils in vitro, focusing on superoxide production, phagocytosis, bactericidal activity, and chemotaxis, in comparison with peripheral blood neutrophils (PB-Neu's) obtained from healthy subjects.

Methods

Human ES cell culture and EB formation

In all experiments using hESCs, we used KhES-3[15] cells (a kind gift from Dr Nakatsuji; Kyoto University, Kyoto, Japan), which were maintained as previously described.[16] Briefly, KhES-3 colonies were cultured on irradiated mouse embryonic fibroblasts in Dulbecco modified Eagle medium/F12 (Invitrogen, Carlsbad, CA) supplemented with 20% KNOCKOUT serum

Submitted May 31, 2008; accepted March 5, 2009. Prepublished online as *Blood* First Edition paper, March 25, 2009; DOI 10.1182/blood-2008-06-160838.

An Inside *Blood* analysis of this article appears at the front of this issue.

The publication costs of this article were defrayed in part by page charge payment. Therefore, and solely to indicate this fact, this article is hereby marked "advertisement" in accordance with 18 USC section 1734.

replacer (Invitrogen) and 2.5 ng/mL human basic fibroblast growth factor (Invitrogen). The culture medium was replaced daily with fresh medium. Colonies were passaged onto new mouse embryonic fibroblasts every 6 days. To induce the formation of EBs, KhES-3 colonies were picked up using collagenase, and cultured in suspension in nonserum stem cell medium that we previously used in a hematopoietic stem cell expansion protocol.[17] After 24 hours, the colonies formed EBs, which were collected and cultured further for 17 days in Iscove modified Dulbecco medium (IMDM; Invitrogen) containing 15% fetal bovine serum (FBS), 1% nonessential amino acid (Invitrogen), 2 mM L-glutamine, 100 U/mL penicillin, 100 μg/mL streptomycin, and 0.1 mM 2-mercaptoethanol (ME) supplemented with cytokines (25 ng/mL bone morphogenic protein-4 [R&D Systems, Minneapolis, MN], 50 ng/mL stem cell factor [SCF; R&D Systems], 50 ng/mL Flt-3 ligand [R&D Systems], 50 ng/mL interleukin-6 [IL-6]/IL-6 receptor fusion protein [FP6; Kyowa Hakko Kirin, Tokyo, Japan], and 20 ng/mL thrombopoietin [TPO; Kyowa Hakko Kirin]).

Expansion of hematopoietic progenitor cells and terminal differentiation into mature neutrophils on OP9 stromal cells

OP9 cells (a kind gift from Dr Nakano; Osaka University, Osaka, Japan) were irradiated with 20 Gy and plated onto gelatin-coated 6-well tissue culture plates at a density of 1.5×10^5/well. The next day, the EBs (incubated for 18 days after the initiation of suspension culture) were trypsinized and disrupted into single cells. Cells were suspended in the progenitor expansion medium (IMDM supplemented with 10% FBS, 10% horse serum [StemCell Technologies, Vancouver, BC], 5% protein-free hybridoma medium [Invitrogen], 0.1 mM 2-ME, 100 U/mL penicillin, 100 μg/mL streptomycin, 100 ng/mL SCF, Flt-3 ligand, FP6, and 10 ng/mL TPO and IL-3 [R&D Systems]) and plated onto the irradiated OP9 cells (day 0). Each well contained up to 5×10^5 EB-derived cells. The culture medium was replaced with fresh medium on day 4.

On day 7 of the progenitor expansion phase, floating cells were collected, suspended with terminal differentiation medium (IMDM supplemented with 10% FBS, 0.1 mM 2-ME, 100 U/mL penicillin, 100 μg/mL streptomycin, and 50 ng/mL granulocyte colony-stimulating factor [G-CSF; Kyowa Hakko Kirin]), and transferred onto the newly irradiated OP9 cells. The culture medium was replaced with fresh medium on day 10. This terminal differentiation phase culture was continued for 6 or 7 days.

Preparation of normal PB-Neu's and bone marrow mononuclear cells

Human peripheral blood and bone marrow cells were obtained from healthy adult donors after obtaining informed consent in accordance with the Declaration of Helsinki. The institutional review board of the University of Tsukuba approved the use of peripheral blood neutrophils in this research. PB-Neu's were prepared as previously described.[18] The purity of the neutrophils was greater than 90%, with the remaining cells mainly eosinophils. Neutrophils were suspended in Hanks balanced salt solution (HBSS; Invitrogen) containing 0.5% bovine serum albumin (BSA) and placed at 4°C. In some experiments, peripheral blood mononuclear cells (PB-MNCs) were collected from the intermediate layer after centrifugation with Lymphoprep (Axis-shield, Oslo, Norway). Bone marrow cells were directly centrifuged with Lymphoprep, and only mononuclear cells were collected. Bone marrow mononuclear cells (BM-MNCs) were used immediately for RNA extraction.

Wright-Giemsa, myeloperoxidase, and alkaline-phosphatase staining

The morphology and granule characteristics of hESC-derived cells at the indicated days were assessed by Wright-Giemsa staining, comparing them with normal PB-Neu's. Myeloperoxidase and alkaline-phosphatase staining was performed using the New PO-K staining kit and alkaline phosphatase staining kit (MUTO PURE CHEMICALS, Tokyo, Japan). The prepared slides were inspected using an Olympus BX51 microscope equipped with a 100 × /1.30 UPlan objective lens (Olympus, Tokyo, Japan). Images were acquired with an HC-2500 digital camera and Photograb-2500 software (Fujifilm, Tokyo, Japan).

Electron microscopy

After 13 or 14 days culture, the population contained predominantly morphologically mature neutrophils, and was defined as hESC-Neu's. The hESC-Neu's and PB-Neu's were fixed in 2% paraformaldehyde/2.5% glutaraldehyde in 0.1 M phosphate buffered saline (PBS; Invitrogen) for at least 12 hours, and then postfixed in 1% osmium tetroxide in 0.1 M PBS for 2 hours. After fixation, samples were dehydrated in a graded ethanol series, cleared with propylene oxide, and embedded in Epon. Thin sections of cured samples were stained with uranyl acetate and Reynolds lead citrate. The sections were inspected using a transmission electron microscope, H7000 (Hitachi, Tokyo, Japan).

Semiquantitative RT-PCR for lactoferrin

Total RNA was obtained from hESC-derived cells of indicated culture days, PB-Neu's, PB-MNC's, and BM-MNC's using an RNeasy mini kit (QIAGEN, Hilden, Germany), and cDNA was synthesized from each RNA sample using a random primer and SuperScript III (Invitrogen) following the manufacturer's protocol. Semiquantitative polymerase chain reaction (PCR) was performed as previously described.[19] The sequence information of gene-specific primers used in reverse transcription (RT)–PCR and the PCR conditions is available upon request.

Flow cytometric analysis

Surface antigens of hESC-derived cells harvested on the indicated days were analyzed by flow cytometry using fluorescence-activated cell sorting (FACS) Aria (Becton Dickinson Immunocytometry Systems, San Jose, CA). Fc receptors on the cells were blocked with PBS containing 2% FBS and FcR Blocking Reagent (Miltenyi Biotec, Bergisch Gladbach, Germany). Antigens were stained with either fluorescein isothiocyanate (FITC)–conjugated antihuman CD13, CD64, CD11b (Beckman Coulter, Fullerton, CA), or CD14 (BD Pharmingen, San Diego, CA) antibodies; phycoerythrin-conjugated antihuman CD16, CD32, CD33 (Beckman Coulter), CD11b, or CD45 (BD Pharmingen) antibodies; or allophycocyanin-conjugated antihuman CD15, CD117 (BD Pharmingen), CD34, or CD133 (Myltenyi Biotec) antibodies. The negative range was determined by referencing the fluorescence of isotype controls. Dead cells were detected using 7-amino-actinomycin D (Via-Probe; BD Pharmingen).

Apoptosis assay

Neutrophils (hESC-Neu's and PB-Neu's) were suspended in IMDM with 0.5% BSA and incubated in 6-well plates at 37°C with 5% CO_2, with or without 50 ng/mL G-CSF. At the indicated time, neutrophils were harvested, stained with FITC-conjugated Annexin V and propidium iodide (PI) using an Annexin V-FITC Kit (Beckman Coulter), and analyzed by FACS Aria. Cells negative for both Annexin V and PI were judged as live cells.

G-CSF stimulation prior to assessing neutrophil function

Because the functions of hESC-Neu's are modified by G-CSF in the culture medium, we stimulated hESC-Neu's and PB-Neu's (PB-Neu(G+)'s) for 15 minutes at 37°C with 50 ng/mL G-CSF in the reaction medium. As a control, PB-Neu's without G-CSF stimulation (PB-Neu(G−)'s) were prepared. hESC-Neu's, PB-Neu(G+)'s, and PB-Neu(G−)'s were used for functional assays directly without changing the medium.

Detection of reactive oxygen species produced by neutrophils

Neutrophil production of reactive oxygen species was detected by flow cytometry using dihydrorhodamine123 (DHR; Sigma-Aldrich, St Louis, MO) as described previously.[20-22] Briefly, 1×10^5 hESC-Neu's, PB-Neu(G+)'s, or PB-Neu(G−)'s were suspended in 400 μL of the reaction medium (HBSS containing 0.5% BSA) per tube, and 3 tubes were prepared of each sample. Catalase (Sigma-Aldrich) at a final concentration of 1000 U/mL, 1.8 μL 29 mM DHR, and 100 μL 3.2 μM phorbol myristate

acetate (PMA; Sigma-Aldrich) were added to 1 of the 3 tubes; either no DHR or only DHR was added in the other 2 tubes as controls. Reaction medium was added to bring the final volume up to 500 μL. After 15-minute reaction at 37°C, the samples were washed twice with ice-cold reaction medium, and suspended in 200 μL reaction medium. Rhodamine fluorescence from the oxidized DHR was detected using FACS Aria.

Phagocytosis and NBT-reduction test using NBT-coated yeast cells

Phagocytosis and NBT reduction were visualized in a single set of experiments. Autoclaved Baker yeast was suspended in 0.5% NBT solution (0.5% NBT [Sigma-Aldrich] and 0.85% sodium chloride in distilled water) at a density of 1×10^8/mL. A 5-μL aliquot of this yeast suspension was added to hESC-Neu's, PB-Neu(G+)'s, and PB-Neu(G−)'s at 2.5×10^5 in 50 μL FBS. After 1 hour at 37°C, the samples were washed and stained with 1% safranin-O (MUTO PURE CHEMCALS) for 5 minutes. The samples were then washed twice and suspended in 100 μL PBS. A small aliquot of each sample was placed onto a glass slide and topped with a cover glass, and the number of ingested yeast cells and their change in color from brown to purple or black were examined using a microscope. Ingested yeast cells that changed color in the cells were counted as NBT-reaction positive, whereas those that were ingested but did not change color were counted as NBT-reaction negative. The phagocytosis rate was calculated as the percentage of neutrophils that contained one or more NBT-positive yeast cells. The phagocytosis score was calculated as the total number of positive yeast cells in 100 neutrophils. Only morphologically determined neutrophils were scored, excluding contaminating cells such as macrophages, the percentage of which was less than 15% of the total cells.

Bacterial killing assay

The bacterial killing assay was performed using *Escherichia coli* ATCC25922 as previously described[23] with some modifications. Briefly, 1×10^8 colony-forming units (CFUs) of exponentially growing bacteria were suspended in 1 mL HEPES-buffered saline with 10% human AB serum (MP Biomedicals, Irvine, CA) and opsonized at 37°C for 30 minutes. Neutrophils (hESC-Neu's, PB-Neu(G−)'s, and PB-Neu(G+)'s) were suspended in HEPES-buffered saline with 40% human AB serum at a concentration of 5×10^6/mL. The opsonized *E coli* was added to the suspension of hESC-Neu's and PB-Neu's, at a neutrophil/bacteria ratio of 2:1, or control medium. After 1-hour incubation, 50 μL of samples with and without neutrophils were diluted in 2.5 mL alkalinized water (pH 11) for lysis of neutrophils. Samples were further diluted with PBS, and duplicate aliquots were added to molten tryptic soy broth with 1.5% agar kept at 42°C, rapidly mixed, and plated on dishes. The CFUs were counted after overnight incubation.

Chemotaxis assay

Chemotactic ability was determined using a modified Boyden chamber method.[24] Briefly, 700 μL of the reaction medium (HBSS containing 0.5% BSA) with or without 10^{-7} M formyl-Met-Leu-Phe (fMLP; Sigma-Aldrich) was placed into each well of a 24-well plate, and the cell culture insert (3.0-μm pores; Falcon; Becton Dickinson, Franklin Lakes, NJ) was gently placed into each well to divide the well into upper and lower sections. Neutrophils were suspended in the reaction medium at 2.5×10^6/mL and 200 μL cell suspension was added to the upper well, allowing the neutrophils to migrate from the upper to the lower side of the membrane for 90 minutes at 37°C. After incubation, the membranes were washed, fixed with methanol, stained with Carrazi hematoxylin (MUTO PURE CHEMICALS), and mounted on the slide glass. The number of neutrophils that migrated through the membrane from the upper to the lower side was counted using a microscope with a high-power lens (× 400) in 3 fields: 2 near the edge and 1 on the center. Only mature neutrophils were counted.

Statistical analyses

Results are expressed as mean plus or minus SD. Statistical significance was determined using a 2-tailed Student *t* test. Results were considered significant when *P* values were less than .05.

Results

Effective derivation of mature neutrophils from hESCs with high purity

After initiating the suspension culture of EB-derived cells, small clusters of round-shaped cells appeared on the OP9 stromal layer around day 4. The morphology of the day-7 cells visualized with Wright-Giemsa staining suggested that they were myeloblasts and promyelocytes. On days 9 and 11, myelocytes and metamyelocytes were predominant, and on day 13 or 14, 70% to 80% of the cells appeared to be stab and segmented neutrophils (Figure 1A), with approximately 90% of the granulocytes at the metamyelocyte stage or later (Table 1). This finding indicated that hESC-derived cells differentiated into mature neutrophils by a process similar to physiologic granulopoiesis. The remaining cells appeared to be macrophages or monocytes, and cells of other lineages, such as erythroid or lymphoid cells, were not observed at any time during the culture. The number of total cells peaked around days 9 to 11, with an average 2.9-fold increase (range; 0.5- to 10.0-fold in 23 independent cultures) compared with the initial EB-derived cell number. The final yield of the cells on day 13 or 14 was 1.7-fold (range; 0.1- to 8.8-fold in 28 independent cultures). We attempted to further purify the hESC-derived mature neutrophils from the "hESC-Neu" population using density gradient methods, but higher purification could not be achieved without massively reducing the cell yield. We therefore used hESC-Neu's in the subsequent experiments.

Most (97.3% ± 1.5%) of the hESC-derived mature neutrophils defined by Wright-Giemsa staining were positive for myeloperoxidase, and the alkaline-phosphatase score of hESC-Neu's was 284 plus or minus 8.6 (Figure 1B). Under transmission electron microscopy, segmented nuclei and round cytoplasmic granules of hESC-Neu's appeared very similar to those in PB-Neu's (Figure 1C).

Some myeloid cell lines, such as HL-60, have abnormal biosynthesis of secondary granule proteins.[25,26] Thus, it is important to verify the biosynthesis of secondary granule proteins in hESC-Neu's. The levels of lactoferrin mRNA in hESC-derived cells at different stages were compared with those in PB-Neu's and BM-MNCs by semiquantitative RT-PCR (Figure 1D). Lactoferrin biosynthesis begins at the myelocyte stage and terminates by the beginning of the band stage.[25,27] Lactoferrin mRNA was not detected in PB-Neu's from some donors, but was detected in PB-Neu's from others. Human ESC–derived cells at various stages as well as BM-MNCs expressed lactoferrin mRNA. The expression level of lactoferrin mRNA in the hESC-derived cells was highest at day 10 of the induction culture and declined on days 13 and 14. These findings are consistent with the documented pattern of lactoferrin biosynthesis.

Surface antigen presentation in comparison to PB-Neu's

Surface antigen expression at each level of differentiation of hESC-derived cells was analyzed by flow cytometry (Figure 2). From days 7 to 13, the common blood cell antigen CD45 was expressed in almost all the cells. CD34, CD117, and CD133, cell surface markers on normal immature hematopoietic cells, were detected in a small population of the cells on day 7, but disappeared by day 10. Common myeloid antigens CD33 and CD15 were also highly expressed, whereas CD11b expression increased during the course of maturation. CD13 is also a common myeloid antigen, but

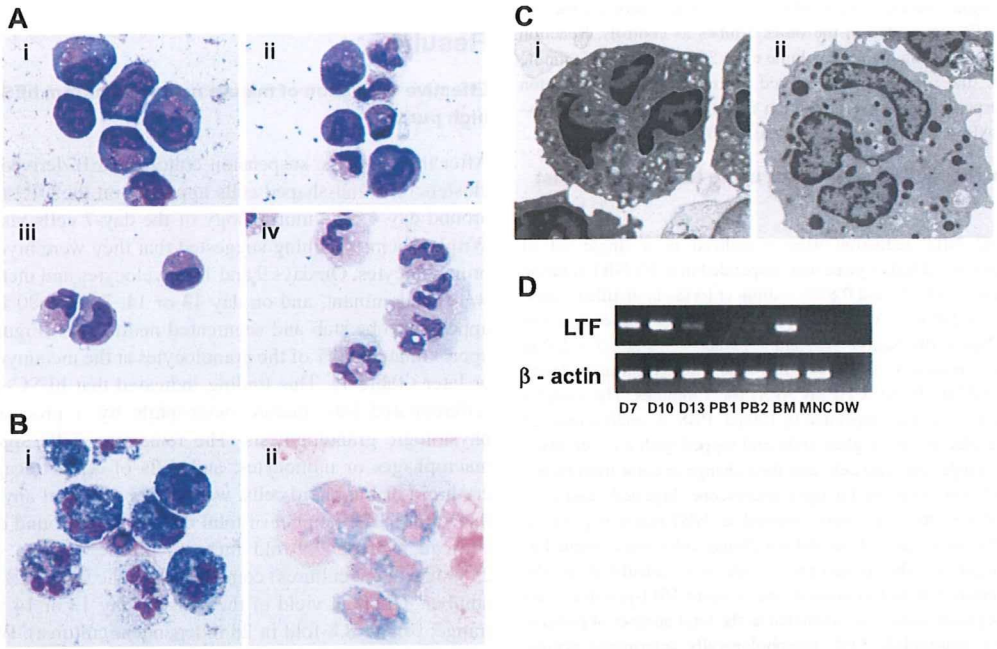

Figure 1. Morphology of hESC-derived cells and expression of lactoferrin mRNA. (A) Wright-Giemsa staining of the day-7 cells (i) revealed that they were morphologically myeloblasts and promyelocytes. On days 9 (ii) and 11 (iii), myelocytes and metamyelocytes were predominant, and on day 13 (iv; hESC-Neu), 70% to 80% of the cells appeared to be stab and segmented neutrophils. Original magnification, ×1000. (Bi) 97.3% plus or minus 1.5% of hESC-Neu's were myeloperoxidase positive. (ii) The neutrophil alkaline-phosphatase score in hESC-Neu's was 284 plus or minus 8.6. Values represent mean plus or minus SD. Original magnification, ×1000. (C) Microstructure of hESC-Neu's. Similar to steady-state neutrophils separated from peripheral blood (i), segmented nuclei and cytoplasmic granules were observed in hESC-Neu's (ii). Original magnification, ×8000. (D) Lactoferrin (LTF) mRNA was expressed in hESC-derived cells on day 7 (D7), peaked on day 10 (D10), and was weakly positive on day 13 (D13). Bone marrow mononuclear cells (BM) were strongly positive for LTF mRNA, but PB-Neu's (PB1 and 2) were negative, although faint bands were detected in PB-Neu's prepared from some donors (data not shown). As a negative control, peripheral blood mononuclear cells (MNCs) were used.

its expression was observed in less than 20% of the cells on day 7 and did not subsequently increase. CD16 (Fcγ receptor (FcγR) III), which is expressed in neutrophils as well as natural killer cells, macrophages, and a small subset of monocytes,[28] was already expressed by day 7, and increased with maturation. This expression pattern of CD16 is consistent with that during normal neutrophil differentiation, although the proportion of $CD16^+$ cells was lower than that of morphology-defined mature neutrophils on day 13. The ratio of CD32 (FcγRII)–positive cells increased as the differentiation stage advanced, and eventually reached 90%. CD64 (FcγRI) expression was greater than 80%, peaking on day 10, and the high percentage was maintained through day 13. CD14 was expressed in 20% to 25% of the cells on days 10 and 13.

Table 1. Differentiation pattern of hESC-derived cells

Cell type	% of total cells		
	Day 7	Day 10	Day 13
Myeloblasts	61.0 ± 9.1	2.3 ± 1.2	ND
Promyelocytes	16.8 ± 6.3	8.5 ± 0.9	0.7 ± 0.8
Myelocytes	12.3 ± 4.8	34.0 ± 6.8	6.4 ± 3.4
Metamyelocytes	3.0 ± 1.0	19.0 ± 1.3	10.2 ± 4.3
Stab neutrophils	0.8 ± 0.3	16.2 ± 3.0	18.3 ± 2.6
Segmented neutrophils	0.3 ± 0.6	14.7 ± 6.0	53.1 ± 9.6
Macrophage/monocytes	5.7 ± 0.6	5.3 ± 1.3	11.2 ± 1.4
Mature neutrophils	1.2 ± 0.8	30.8 ± 4.6	71.4 ± 7.4

The sum of the stab and segmented neutrophils indicates the total mature neutrophils. Data are shown as mean plus or minus SD (n = 3 independent experiments).

ND indicates not detectable.

In normal peripheral blood, both neutrophils and monocytes express CD15 and CD11b. In addition, mature neutrophils express CD16, whereas monocytes express CD14.[28,29] Detailed analysis on day 13 revealed that approximately 70% of $CD15^+$ and $CD11b^+$ cells were $CD16^+$, and almost all $CD15^+$ and $CD16^+$ cells expressed CD11b (Figure 2Bi,ii). Given that 70% to 80% of the cells on day 13 were morphologically mature neutrophils (Table 1), it is likely that the majority of hESC-Neu's had CD15, CD11b, and CD16 expression patterns similar to PB-Neu's, although some hESC-Neu's did not express CD15 or CD16, particularly CD16.

CD32 is broadly expressed on myeloid cells, whereas CD64 is expressed only on monocytes but not on neutrophils in the peripheral blood.[28] In the bone marrow, CD64 expression is observed in a small population of myeloblasts, peaks at the promyelocyte, myelocyte, and metamyelocyte stages, and then diminishes, although a small proportion of the stab neutrophils still express CD64.[30,31] We confirmed that virtually no PB-Neu's expressed CD64 (data not shown). In contrast, almost all $CD15^+$ and $CD16^+$ hESC-Neu's expressed CD64 on day 13, indicating that both stab and segmented hESC-Neu's expressed CD64, because segmented neutrophils represented more than 50% of the cells on day 13 (Figure 2Biii; Table 1). Nearly 50% of $CD15^+$ and $CD16^+$ cells were weakly positive for CD14, in contrast to the negative expression of CD14 in steady-state PB-Neu's (Figure 2Biv). This aberrant expression of CD64 and CD14 in hESC-Neu's is similar to their positive expression on some of the neutrophils harvested from healthy donors who received G-CSF administration[32,33] and the neutrophils derived from bone marrow $CD34^+$ cells in vitro by G-CSF stimulation.[31]

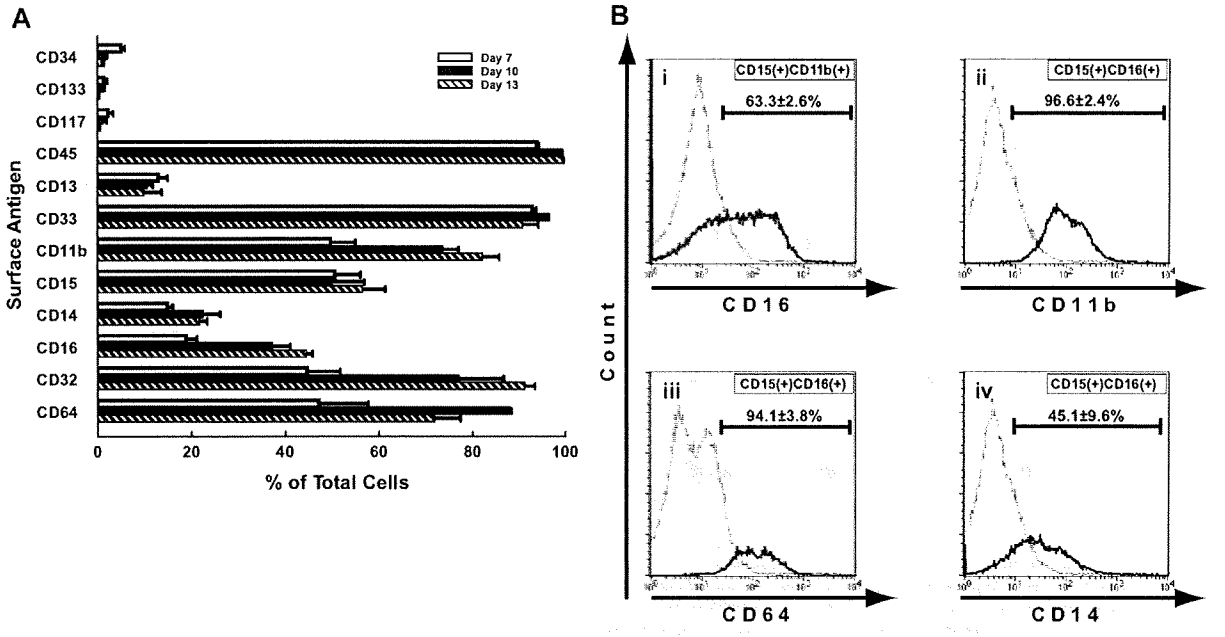

Figure 2. Surface antigens of hESC-derived cells. (A) Surface antigen expression at each level of differentiation of hESC-derived cells was analyzed by flow cytometry. CD45 was expressed in almost all the cells. CD34, CD117, and CD133, immature markers of hematopoiesis, were detected in a small population of the cells on day 7, and had almost disappeared by day 10. Common myeloid antigens CD33 and CD15 were highly expressed, and the expression of CD11b increased during maturation. CD13 was expressed in less than 20% of the cells throughout the culture period. The expression of CD16, a mature neutrophil marker, increased following maturation, but was observed in only approximately 45% of the cells, even on day 13. CD14 and CD64 expression was aberrantly observed in some cells. Bars represent SDs (n = 3). (B) In the steady state, mature neutrophils in peripheral blood were $CD15^+$, $CD11b^+$, and $CD16^+$. (i) In hESC-derived cells on day 13, 63.3% plus or minus 2.6% of the $CD15^+$ and $CD11b^+$ cells were $CD16^+$, and (ii) almost all of the $CD15^+$ and $CD16^+$ cells were $CD11b^+$. (iii-iv) On the other hand, CD64 and CD14 were rarely expressed on mature neutrophils in the peripheral blood. $CD15^+$ and $CD16^+$ cells from hESCs, consistent with the phenotype of mature neutrophils, showed aberrant expression of CD64 (iii) and CD14 (iv), in 94.1% plus or minus 3.8% and 45.1% plus or minus 9.6% of the cells, respectively. Data are presented as mean plus or minus SD (n = 3).

Apoptosis pattern and prolonged survival by G-CSF of hESC-Neu's and PB-Neu's

In the steady state, PB-Neu's have a short life span of approximately 24 hours, but this can be prolonged by G-CSF stimulation.[34] Some hESC-Neu's were already apoptotic at the time of harvest and therefore we focused on the nonapoptotic fraction of hESC-Neu's (Figure 3). In contrast to the PB-Neu's, which underwent apoptosis within 6 hours without G-CSF, consistent with previous reports,[34] a proportion of apoptotic cells among hESC-Neu's in the medium without G-CSF did not increase for up to 6 hours after the start of the culture. In addition, there were no differences between the cultures with and without G-CSF for up to 6 hours. After 6 hours, however, there was a more rapid decrease in nonapoptotic cells in hESC-Neu's without G-CSF than in hESC-Neu's with G-CSF, which resulted in a lower number of viable cells than hESC-Neu's with G-CSF at 24 hours, although the number of viable cells of hESC-Neu's without G-CSF was still higher than that of PB-Neu's without G-CSF.

Oxidative burst phenotype was similar in hESC-Neu's and PB-Neu's

Oxidative burst is an essential function of neutrophils when killing microorganisms, but an inappropriate burst sometime causes injury to the host tissue. We assessed the ability to convert DHR to rhodamine in hESC-Neu's and PB-Neu's using flow cytometry.[20] Because G-CSF, which could substantially affect the result, was used during the culture, we compared hESC-Neu's with PB-Neu(G+)'s and PB-Neu(G−)'s as described in "G-CSF stimulation prior to assessing neutrophil function." When DHR was added to the neutrophil suspensions, rhodamine-specific fluorescence was detected in hESC-Neu's, and in PB-Neu(G−)'s and PB-Neu(G+)'s without PMA stimulation, indicating basal superoxide production without PMA stimulation in each neutrophil preparation (Figure 4). PMA stimulation increased rhodamine mean fluorescence intensity in hESC-Neu's, but to a lesser extent than in PB-Neu(G−)'s and PB-Neu(G+)'s. Consequently, the mean rhodamine fluorescence intensity after PMA stimulation was similar in hESC-Neu's, PB-Neu(G−)'s, and PB-Neu(G+)'s, suggesting that the maximum superoxide production is comparable between hESC-Neu's and PB-Neu's.

Phagocytosis and subsequent NBT reduction activity, and bactericidal activity were similar between hESC-Neu's and PB-Neu's

Neutrophils protect against infectious microorganisms by phagocytosing and subsequently killing them. These functions of hESC-Neu's and PB-Neu's were evaluated in an experimental system using NBT-coated yeast. Under the microscope, mature neutrophils could be easily distinguished from contaminating macrophages by the unique shape of their nuclei after 1% safranin-O staining (Figure 5A). NBT-coated yeast that had not been ingested had a red-brown color that began to change to purple or black, beginning at the periphery, and eventually became completely black, because the NBT coating on the yeast was reduced by neutrophils after phagocytosis. Thus, neutrophils that had phagocytosis and NBT-reducing ability could be easily identified. hESC-Neu's had a slightly lower phagocytosis rate than PB-Neu(G−)'s and PB-Neu(G+)'s (Figure 5B). The phagocytosis score, however, was not significantly different between hESC-Neu's and PB-Neu(G−)'s and PB-Neu(G+)'s (Figure 5C). The cells on day 8 of the culture, most of which were morphologically myeloblasts and promyelocytes, were rarely observed

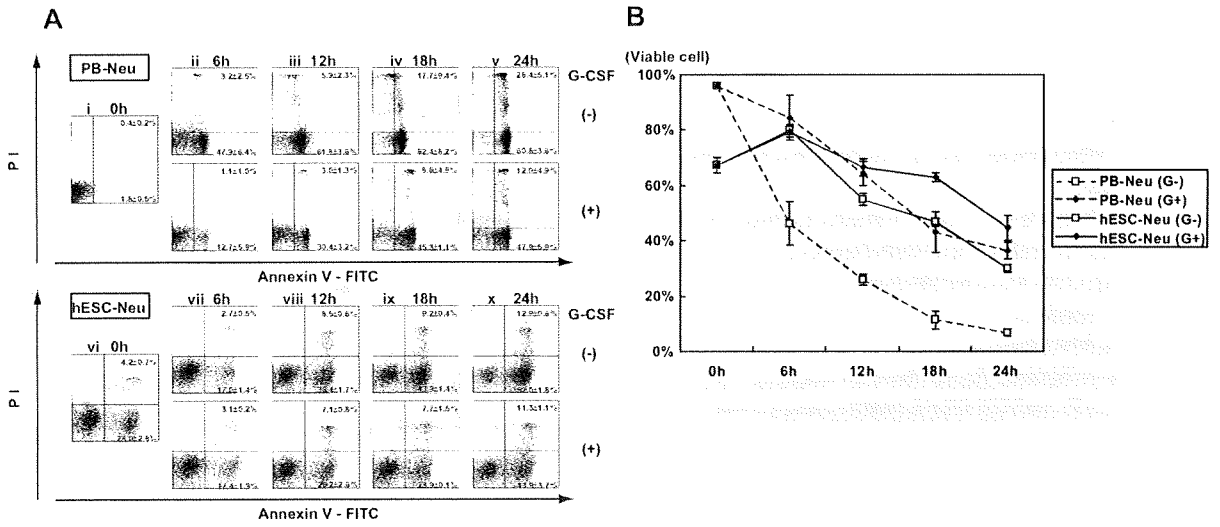

Figure 3. Apoptosis pattern and G-CSF effect on survival of hESC-Neu's. (A) Flow cytometric analysis. In the steady state, PB-Neu's have a short life span of approximately 24 hours, but this can be prolonged by G-CSF stimulation (i-v). Some hESC-Neu's were already apoptotic at the time of the harvest from the induction culture (vi). In contrast to the PB-Neu's that underwent apoptosis within 6 hours without G-CSF (ii), the proportion of apoptotic cells did not increase for up to 6 hours after the start of the culture of hESC-Neu's in the medium without G-CSF (vi,vii). In addition, there were no differences between the cultures of hESC-Neu's with and without G-CSF for up to 6 hours (vii). After 6 hours, nonapoptotic cells decreased more rapidly among hESC-Neu's without G-CSF than among hESC-Neu's with G-CSF (viii-x), resulting in the lower number of viable cells than hESC-Neu's with G-CSF at 24 hours (x). Figures are representative of 3 independent experiments. Data are presented as mean plus or minus SD (n = 3). (B) The time course of the decrease in viable cells. Bars represent SDs (n = 3).

to phagocytose the yeast or reduce NBT if they had ingested the yeast, indicating that we observed phagocytosis and NBT reduction that was specific to mature neutrophils.

Because the hESC-Neu's had sufficient phagocytosing ability and superoxide production, we next investigated whether hESC-Neu's can kill bacteria. The bactericidal activity of hESC-Neu's and PB-Neu's was compared using *E coli*. When incubated with hESC-Neu's and PB-Neu(G−)'s and PB-Neu(G+)'s, the numbers of CFUs were similarly reduced to approximately 40% that of the control, indicating comparable bactericidal activity against *E coli* between hESC-Neu's and PB-Neu's (Figure 5D).

Chemotaxis was similar between hESC-Neu's and PB-Neu's

We compared chemotaxis of hESC-Neu's and PB-Neu's using a modified Boyden chamber method. After incubation with or without fMLP in the lower well, neutrophils had migrated from the upper side to the lower side of the membrane. Neutrophil migration without fMLP in the lower well was considered random migration. The number of neutrophils that migrated randomly was not significantly different between hESC-Neu's and PB-Neu(G−)'s, but PB-Neu(G+)'s showed significantly more random migration than the others (Figure 5E). The number of migrated cells increased in hESC-Neu's, PB-Neu(G−)'s, and PB-Neu(G+)'s when fMLP was added in the lower well. The increase in cell migration induced by chemotaxis to fMLP was calculated by subtracting the number of randomly migrated cells without fMLP from that of migrated cells with fMLP. There were no significant differences between hESC-Neu's and PB-Neu(G−)'s or PB-Neu(G+)'s in the net fMLP-induced chemotaxis.

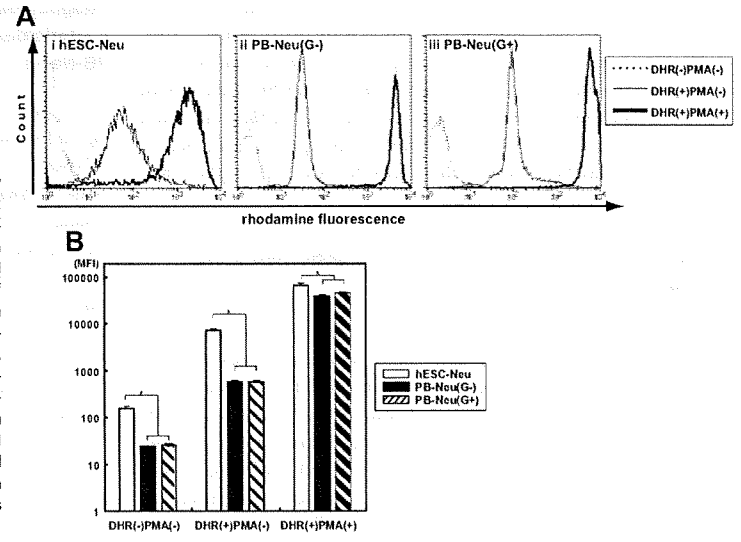

Figure 4. Superoxide production of hESC-Neu's assessed by dihydrorhodamine123 oxidation. (A) Dihydrorhodamine123 (DHR) was reacted to neutrophils with or without phorbol myristate acetate (PMA), and the resultant rhodamine fluorescence was detected by flow cytometry. When DHR was added to the reaction medium without PMA (line), the fluorescence levels were slightly elevated in hESC-Neu's (i), PB-Neu(G−)'s (ii), and PB-Neu(G+)'s (iii). The addition of PMA dramatically increased the levels of fluorescence in all 3 neutrophil preparations (bold line). The figures are representative of 3 independent experiments. (B) Comparison of superoxide production between hESC-Neu's and PB-Neu's using mean fluorescence intensity (MFI) of rhodamine. When DHR was added without PMA stimulation, rhodamine-specific fluorescence was detected in hESC-Neu's, PB-Neu(G−)'s, and PB-Neu(G+)'s. PMA stimulation increased rhodamine MFI in hESC-Neu's though to a lesser extent than in PB-Neu(G−)'s and PB-Neu(G+)'s. Consequently, rhodamine MFI after PMA stimulation was similar in hESC-Neu's, PB-Neu(G−)'s, and PB-Neu(G+)'s, suggesting that the maximum superoxide production was comparable between hESC-Neu's and PB-Neu's (n = 3; bars represent SDs; $^*P < .05$ compared with hESC-Neu's).

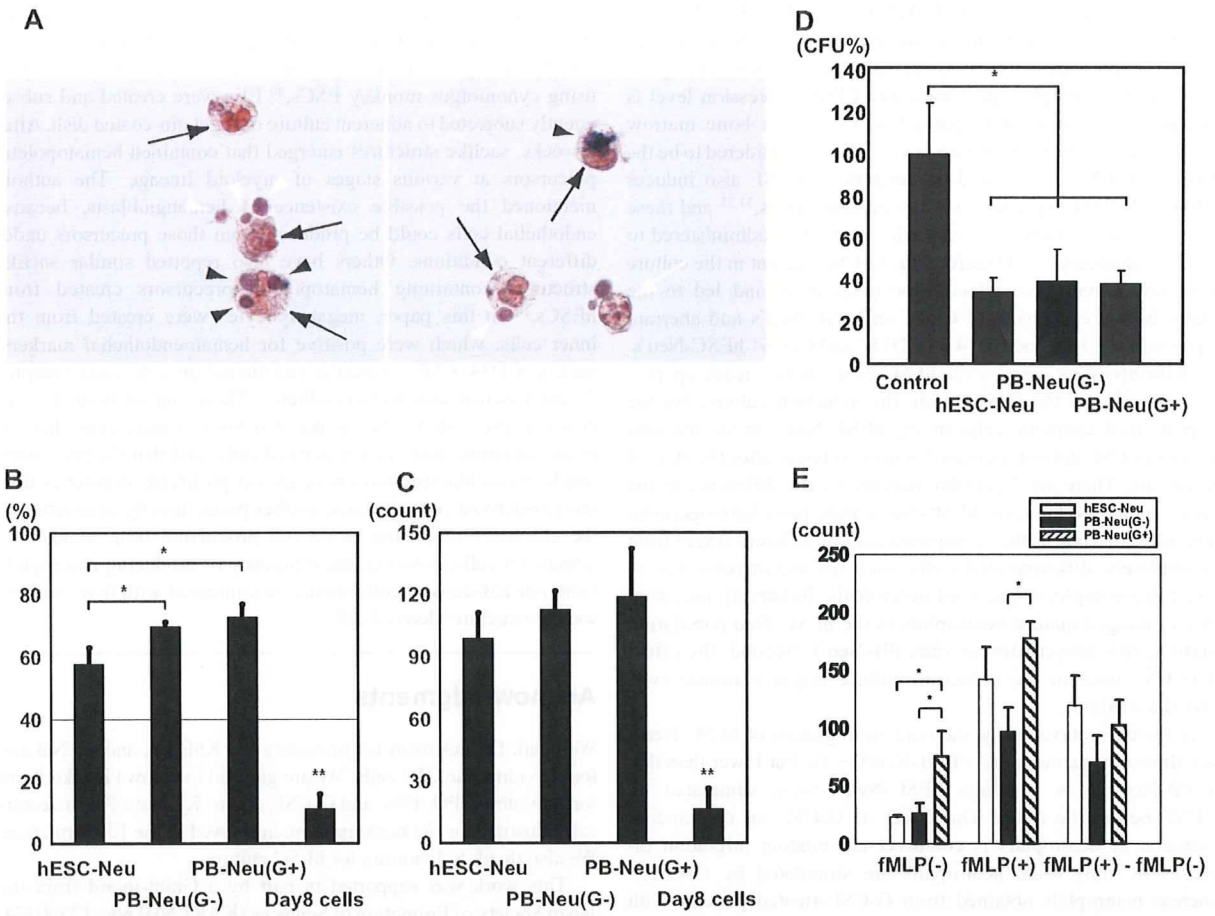

Figure 5. NBT-coated yeast cell-phagocytosis test, bactericidal activity, and chemotaxis assay. (A) NBT-coated yeast cells were added to a neutrophil suspension and incubated at 37°C. After 1 hour, the cells were stained with 1% safranin-O, and observed using a microscope. Mature neutrophils (→) could be easily distinguished from contaminating macrophages (white arrow; only the nucleus is observed in the figure) by the unique shape of their nuclei. Yeast cells were red-brown in color before being ingested (white arrowhead); the color began to change to purple or black beginning at the periphery of the yeast cell, and eventually became completely black (➤) because the NBT was reduced after ingestion. Yeast cells that changed color in the cells were counted as NBT-reduction positive. Original magnification, ×400. (B) The phagocytosis rate was calculated as a percentage of the neutrophils that contained one or more yeast cells. hESC-Neu's had a slightly lower phagocytosis rate than that of PB-Neu(G−)'s and PB-Neu(G+)'s. (C) The phagocytosis score was calculated as the total number of positive yeast cells in 100 neutrophils. There were no significant differences in the phagocytosis score between hESC-Neu's and PB-Neu(G−)'s or PB-Neu(G+)'s. The cells on day 8 of the culture (day-8 cells) were rarely observed to phagocytose the yeast cells or reduce NBT. (In B-C, n = 3; bars indicate SDs; $^{*}P < .05$ compared with PB-Neu(G−)'s and PB-Neu(G+)'s; $^{**}P < .05$ compared with hESC-Neu's, PB-Neu(G−)'s, and PB-Neu(G+)'s.) (D) Bactericidal assay. *E coli* was opsonized with human AB serum, and incubated with hESC-Neu's, PB-Neu(G−)'s, PB-Neu(G+)'s, or control medium. After 1-hour incubation with hESC-Neu's, PB-Neu(G−)'s, and PB-Neu(G+)'s, the colony-forming units (CFUs) were significantly reduced to approximately 40% of the control. There were no significant differences in bactericidal activity between hESC-Neu's, PB-Neu(G−)'s, and PB-Neu(G+)'s. The CFUs of controls are presented as 100% (n = 3; bars indicate SDs; $^{*}P < .05$ compared with control). (E) Chemotaxis assay by a modified Boyden chamber method. The number of neutrophils that migrated randomly (fMLP(−)) was not significantly different between hESC-Neu's and PB-Neu(G−)'s, but PB-Neu(G+)'s showed significantly greater random migration than hESC-Neu's and PB-Neu(G−)'s. The number of migrating cells increased in all hESC-Neu's, PB-Neu(G−)'s, and PB-Neu(G+)'s when fMLP was added to the lower well (fMLP(+)). The increase in the number of migrating cells induced by chemotaxis to fMLP (fMLP(+)-fMLP(−)) was not significantly different between hESC-Neu's and PB-Neu(G−)'s or PB-Neu(G+)'s (n = 3; bars indicate SDs; $^{*}P < .05$).

Discussion

We developed a specific and effective method for deriving mature neutrophils from hESCs, making it possible to analyze hESC-derived neutrophils in detail. hESC-derived neutrophils had characteristics similar to steady-state peripheral blood mature neutrophils in morphology and essential functions, although there were some differences in surface antigen expression.

Unfortunately, attempts to further purify the hESC-derived mature neutrophils from the hESC-Neu population by density gradient methods led to a massive reduction in cell yield. In the flow cytometric analysis, the mean intensity of hESC-Neu's in forward scatter was higher than that of PB-Neu's (data not shown), indicating that the size of morphologically mature neutrophils, comprising 70% to 80% of the hESC-Neu population, was larger than that of PB-Neu's. This finding indicates that the density of morphologically mature neutrophils in the hESC-Neu population was lower than that of PB-Neu's, which made it difficult to separate hESC-Neu's from other contaminating cells.

In this culture, we observed morphologically defined myeloblasts, promyelocytes, myelocytes, metamyelocytes, and, eventually, mature stab and segmented neutrophils, in this order, during the 13-day culture, which is similar to the granulocyte maturation process in bone marrow. The surface antigen expression pattern during differentiation was similar to that during normal granulopoiesis, with CD34 and CD117 expression on immature cells, and an increase in CD16 expression as differentiation advanced. Most

hESC-Neu's expressed CD16, CD15, CD11b, CD33, and CD45. This pattern is consistent with normal PB-Neu's, but the percentage of CD16-expressing cells was lower than that of mature neutrophils determined by morphology. The lower CD16 expression level is documented in neutrophils derived in vitro from bone marrow $CD34^+$ cells by stimulation with G-CSF, and is considered to be the effect of G-CSF on myeloid progenitors.[31] G-CSF also induces CD64 and CD14 expression on mature neutrophils,[31,35] and these effects are also observed in vivo when G-CSF is administered to healthy volunteers.[32,33] Therefore, the G-CSF present in the culture from day 7 may have affected the progenitors and led to the relatively low expression of CD16 on hESC-Neu's and aberrant expression of CD64 and CD14 on $CD15^+$ and $CD16^+$ hESC-Neu's.

In the apoptosis assay, some hESC-Neu's were already apoptotic at the time of the harvest from the induction culture, but the proportion of apoptotic cells among hESC-Neu's in the medium without G-CSF did not increase for up to 6 hours after the start of the culture. There are 2 possible reasons for the difference in the rate of apoptosis. First, the hESC-Neu's were more heterogeneous than the PB-Neu's, as they comprised cells at different stages from incompletely differentiated cells such as metamyelocytes to maturation-completed and aged neutrophils. Relatively immature cells or unaged mature neutrophils in the hESC-Neu population might have a longer lifespan than PB-Neu's. Second, the effect of G-CSF used in the induction culture might continue even after the washout.

In the chemotaxis assay, the random migration of hESC-Neu's was almost the same as that of PB-Neu(G−)'s, but lower than that of PB-Neu(G+)'s, although hESC-Neu's were stimulated by G-CSF before the assay. The effect of G-CSF on the random migration of neutrophils is controversial; random migration increases in vitro when neutrophils are stimulated by G-CSF,[36] whereas neutrophils obtained from G-CSF–treated patients with nonmyeloid malignancies show decreased random migration and chemotaxis.[37,38] Our in vitro experiment with PB-Neu(G+)'s and PB-Neu(G−)'s replicated the former result. Nevertheless, hESC-Neu's showed relatively low random migration despite stimulation with G-CSF, while maintaining almost normal fMLP-induced chemotaxis. One possible reason for these differences might be the continuous stimulation by G-CSF; hESC-Neu's were stimulated from the myeloblast stage, and thus, it was expected that the characteristics of the hESC-Neu's were more similar to those of neutrophils from G-CSF–stimulated donors rather than to normal mature neutrophils.

The low yield of hESC-Neu's is a major obstacle to their functional analysis in animals, and further, to their potential use in drug screening and clinical applications. The number of hESC-Neu's produced was less than twice that of the input EB-derived cells. Recently, erythroid progenitor cell lines that could differentiate into functional mature red blood cells both in vitro and in vivo were established from mouse ESCs.[39] In that report, the starting number of ESCs required to establish one progenitor line was 5×10^5, and transplantation of 2×10^7 cells of the progenitor line could ameliorate anemia in mice by increasing the red blood cell count. Similar methods could be considered in the granulopoiesis from hESCs. Another potential method is to use more immature or proliferation-competent cells than the cells with which we initiated the induction culture. One candidate may be hematopoietic progenitors that emerge in saclike structures derived from ESCs. In a report using cynomolgus monkey ESCs,[40] EBs were created and subsequently subjected to adherent culture on a gelatin-coated dish. After 2 weeks, saclike structures emerged that contained hematopoietic precursors at various stages of myeloid lineage. The authors mentioned the possible existence of hemangioblasts, because endothelial cells could be produced from those precursors under different conditions. Others have also reported similar saclike structures containing hematopoietic precursors created from hESCs.[10] In this paper, megakaryocytes were created from the inner cells, which were positive for hematoendothelial markers, such as CD34, CD31, vascular endothelial growth factor-receptor 2, and vascular endothelial-cadherin. These similar findings suggest that the cells in the saclike structures contain cells that are more immature than our EB-derived cells, and that the precursors inside the saclike structures have greater proliferation potency than our EB-derived cells. Because neither paper directly demonstrated the efficiency of mature blood cell production from monkey or human ES cells, however, the efficiency of producing neutrophils from our EB-derived cells should be compared with that from the saclike structure–derived cells.

Acknowledgments

We thank Dr Nakatsuji for providing the KhES-3, and Dr Nakano for providing the OP9 cells. We are grateful to Kyowa Hakko Kirin for providing TPO, FP6, and G-CSF, and to Kyokuto Pharmaceutical Industrial for the nonserum medium used in the EB formation. We also thank S. Ichimura for hESC culture.

This work was supported in part by a Grant-in-aid from the Japan Society of Promotion of Sciences (KAKENHI nos. 17390274, 18013012, 19390258, and 20015010); Research on Pharmaceutical and Medical Safety, Health and Labor Sciences Research Grants from the Ministry of Health, Labor and Welfare of Japan (H16-Iyaku-32); grants from the Astellas Foundation for Research on Metabolic Disorders; the Uehara Memorial Foundation; and the Sagawa Foundation for Promotion of Cancer Research (S.C.); and the Project for Realization of Regenerative Medicine (S.O.).

Authorship

Contribution: Y.Y. and T.S. performed the experiments; K.H. designed the NBT-coated yeast cell-phagocytosis test; M.S.-Y., and K.K. assisted with interpretation of experiments and provided insightful comments; Y.Y. interpreted the data, made the figures, and wrote the paper; T.T., M.K., and S.O. advised on experimental design; S.C. provided critical reading of the paper; T.S. and S.C. designed the research.

Conflict-of-interest disclosure: The authors declare no competing financial interests.

Correspondence: Shigeru Chiba, Department of Clinical and Experimental Hematology, University of Tsukuba, 1-1-1 Tennodai, Tsukuba, Ibaraki, 305-8575, Japan; e-mail: schiba-tky@umin.net.

References

1. Kaufman DS, Hanson ET, Lewis RL, Auerbach R, Thomson JA. Hematopoietic colony-forming cells derived from human embryonic stem cells. Proc Natl Acad Sci U S A. 2001;98:10716-10721.
2. Nakano T, Kodama H, Honjo T. Generation of lymphohematopoietic cells from embryonic stem cells in culture. Science. 1994;265:1098-1101.
3. Vodyanik MA, Bork JA, Thomson JA, Slukvin II. Human embryonic stem cell-derived CD34+ cells: efficient production in the coculture with OP9 stromal cells and analysis of lymphohematopoietic potential. Blood. 2005;105:617-626.

4. Chadwick K, Wang L, Li L, et al. Cytokines and BMP-4 promote hematopoietic differentiation of human embryonic stem cells. Blood. 2003;102: 906-915.
5. Cerdan C, Rouleau A, Bhatia M. VEGF-A165 augments erythropoietic development from human embryonic stem cells. Blood. 2004;103: 2504-2512.
6. Wang L, Menendez P, Shojaei F, et al. Generation of hematopoietic repopulating cells from human embryonic stem cells independent of ectopic HOXB4 expression. J Exp Med. 2005;201:1603-1614.
7. Keller G, Kennedy M, Papayannopoulou T, Wiles MV. Hematopoietic commitment during embryonic stem cell differentiation in culture. Mol Cell Biol. 1993;13:473-486.
8. Wang L, Li L, Shojaei F, et al. Endothelial and hematopoietic cell fate of human embryonic stem cells originates from primitive endothelium with hemangioblastic properties. Immunity. 2004;21: 31-41.
9. Lu SJ, Feng Q, Caballero S, et al. Generation of functional hemangioblasts from human embryonic stem cells. Nat Methods. 2007;4:501-509.
10. Takayama N, Nishikii H, Usui J, et al. Generation of functional platelets from human embryonic stem cells in vitro via ES-sacs, VEGF-promoted structures that concentrate hematopoietic progenitors. Blood. 2008;111:5298-5306.
11. Hübel K, Carter RA, Liles WC, et al. Granulocyte transfusion therapy for infections in candidates and recipients of HPC transplantation: a comparative analysis of feasibility and outcome for community donors versus related donors. Transfusion. 2002;42:1414-1421.
12. Mousset S, Hermann S, Klein SA, et al. Prophylactic and interventional granulocyte transfusions in patients with haematological malignancies and life-threatening infections during neutropenia. Ann Hematol. 2005;84:734-741.
13. Price TH. Granulocyte transfusion: current status. Semin Hematol. 2007;44:15-23.
14. Bhatia M. Hematopoietic development from human embryonic stem cells. Hematology Am Soc Hematol Educ Program. 2007;2007:11-16.
15. Suemori H, Yasuchika K, Hasegawa K, Fujioka T, Tsuneyoshi N, Nakatsuji N. Efficient establishment of human embryonic stem cell lines and long-term maintenance with stable karyotype by enzymatic bulk passage. Biochem Biophys Res Commun. 2006;345:926-932.
16. Thomson JA, Itskovitz-Eldor J, Shapiro SS, et al. Embryonic stem cell lines derived from human blastocysts. Science. 1998;282:1145-1147.
17. Suzuki T, Yokoyama Y, Kumano K, et al. Highly efficient ex vivo expansion of human hematopoietic stem cells using Delta1-Fc chimeric protein. Stem Cells. 2006;24:2456-2465.
18. Yuo A, Kitagawa S, Okabe T, et al. Recombinant human granulocyte colony-stimulating factor repairs the abnormalities of neutrophils in patients with myelodysplastic syndromes and chronic myelogenous leukemia. Blood. 1987;70:404-411.
19. Kumano K, Chiba S, Shimizu K, et al. Notch1 inhibits differentiation of hematopoietic cells by sustaining GATA-2 expression. Blood. 2001;98:3283-3289.
20. Vowells SJ, Sekhsaria S, Malech HL, Shalit M, Fleisher TA. Flow cytometric analysis of the granulocyte respiratory burst: a comparison study of fluorescent probes. J Immunol Methods. 1995; 178:89-97.
21. Richardson MP, Ayliffe MJ, Helbert M, Davies EG. A simple flow cytometry assay using dihydrorhodamine for the measurement of the neutrophil respiratory burst in whole blood: comparison with the quantitative nitrobluetetrazolium test. J Immunol Methods. 1998;219:187-193.
22. Emmendörffer A, Hecht M, Lohmann-Matthes ML, Roesler J. A fast and easy method to determine the production of reactive oxygen intermediates by human and murine phagocytes using dihydrorhodamine 123. J Immunol Methods. 1990; 131:269-275.
23. Decleva E, Menegazzi R, Busetto S, Patriarca P, Dri P. Common methodology is inadequate for studies on the microbicidal activity of neutrophils. J Leukoc Biol. 2006;79:87-94.
24. Harvath L, Falk W, Leonard EJ. Rapid quantitation of neutrophil chemotaxis: use of a polyvinylpyrrolidone-free polycarbonate membrane in a multiwell assembly. J Immunol Methods. 1980;37: 39-45.
25. Rado TA, Bollekens J, St Laurent G, Parker L, Benz EJ Jr. Lactoferrin biosynthesis during granulocytopoiesis. Blood. 1984;64:1103-1109.
26. Rado TA, Wei XP, Benz EJ Jr. Isolation of lactoferrin cDNA from a human myeloid library and expression of mRNA during normal and leukemic myelopoiesis. Blood. 1987;70:989-993.
27. Cowland JB, Borregaard N. The individual regulation of granule protein mRNA levels during neutrophil maturation explains the heterogeneity of neutrophil granules. J Leukoc Biol. 1999;66:989-995.
28. van de Winkel JG, Anderson CL. Biology of human immunoglobulin G Fc receptors. J Leukoc Biol. 1991;49:511-524.
29. van Lochem EG, van der Velden VH, Wind HK, te Marvelde JG, Westerdaal NA, van Dongen JJ. Immunophenotypic differentiation patterns of normal hematopoiesis in human bone marrow: reference patterns for age-related changes and disease-induced shifts. Cytometry B Clin Cytom. 2004;60:1-13.
30. Ball ED, McDermott J, Griffin JD, Davey FR, Davis R, Bloomfield CD. Expression of the three myeloid cell-associated immunoglobulin G Fc receptors defined by murine monoclonal antibodies on normal bone marrow and acute leukemia cells. Blood. 1989;73:1951-1956.
31. Kerst JM, van de Winkel JG, Evans AH, et al. Granulocyte colony-stimulating factor induces hFc gamma RI (CD64 antigen)-positive neutrophils via an effect on myeloid precursor cells. Blood. 1993;81:1457-1464.
32. Kerst JM, de Haas M, van der Schoot CE, et al. Recombinant granulocyte colony-stimulating factor administration to healthy volunteers: induction of immunophenotypically and functionally altered neutrophils via an effect on myeloid progenitor cells. Blood. 1993;82:3265-3272.
33. Carulli G. Effects of recombinant human granulocyte colony-stimulating factor administration on neutrophil phenotype and functions. Haematologica. 1997;82:606-616.
34. van Raam BJ, Drewniak A, Groenewold V, van den Berg TK, Kuijpers TW. Granulocyte colony-stimulating factor delays neutrophil apoptosis by inhibition of calpains upstream of caspase-3. Blood. 2008;112:2046-2054.
35. Kerst JM, Slaper-Cortenbach IC, von dem Borne AE, van der Schoot CE, van Oers RH. Combined measurement of growth and differentiation in suspension cultures of purified human CD34-positive cells enables a detailed analysis of myelopoiesis. Exp Hematol. 1992;20:1188-1193.
36. Nakamae-Akahori M, Kato T, Masuda S, et al. Enhanced neutrophil motility by granulocyte colony-stimulating factor: the role of extracellular signal-regulated kinase and phosphatidylinositol 3-kinase. Immunology. 2006;119:393-403.
37. Azzarà A, Carulli G, Rizzuti-Gullaci A, Minnucci S, Capochiani E, Ambrogi F. Motility of rhG-CSF-induced neutrophils in patients undergoing chemotherapy: evidence for inhibition detected by image analysis. Br J Haematol. 1996;92:161-168.
38. Ribeiro D, Veldwijk MR, Benner A, et al. Differences in functional activity and antigen expression of granulocytes primed in vivo with filgrastim, lenograstim, or pegfilgrastim. Transfusion. 2007; 47:969-980.
39. Hiroyama T, Miharada K, Sudo K, Danjo I, Aoki N, Nakamura Y. Establishment of mouse embryonic stem cell-derived erythroid progenitor cell lines able to produce functional red blood cells. PLoS ONE. 2008;3:e1544.
40. Nakahara M, Matsuyama S, Saeki K, et al. A feeder-free hematopoietic differentiation system with generation of functional neutrophils from feeder- and cytokine-free primate embryonic stem cells. Cloning Stem Cells. 2008;10:341-354.

Molecular allelokaryotyping of T-cell prolymphocytic leukemia cells with high density single nucleotide polymorphism arrays identifies novel common genomic lesions and acquired uniparental disomy

Daniel Nowak,*[1] Emilie Le Toriellec,*[2,3] Marc-Henri Stern,[2,3] Norihiko Kawamata,[1] Tadayuki Akagi,[1] Martin J. Dyer,[4] Wolf-Karsten Hofmann,[5] Seishi Ogawa,[6,7,8] and H. Phillip Koeffler[1]

[1]Division of Hematology and Oncology, Cedars Sinai Medical Center, UCLA School of Medicine, Los Angeles, USA; [2]Institut Curie, Centre de Recherche, Paris, France; [3]Inserm U830, Paris, France; [4]Department of Hematology, University Hospitals, Leicester, United Kingdom; [5]Department of Hematology and Oncology, Charité University Hospital, Campus Benjamin Franklin, Berlin, Germany; [6]Department of Hematology and Oncology and [7]Department of Cell Therapy and Transplantation Medicine and the 21st century COE program, Graduate School of Medicine, University of Tokyo, Japan, and [8]Core Research for Evolutional Science and Technology, Japan Science and Technology Agency, Japan

ABSTRACT

Background

T-cell prolymphocytic leukemia is a rare aggressive lymphoproliferative disease with a mature T-cell phenotype and characteristic genomic lesions such as inv(14)(q11q34), t(14;14)(q11;q32) or t(X;14)(q28;q11), mutation of the *ATM* gene on chromosome 11 and secondary alterations such as deletions of chromosome 8p and duplications of 8q.

Design and Methods

We analyzed malignant cells from 18 patients with T-cell prolymphocytic leukemia using high density 250K single nucleotide polymorphism arrays and molecular allelokaryotyping to refine understanding of known alterations and identify new target genes.

Results

Our analyses revealed that characteristic disruptions of chromosome 14 are frequently unbalanced. In the commonly deleted region on chromosome 11, we found recurrent microdeletions targeting the microRNA 34b/c and the transcription factors *ETS1* and *FLI1*. On chromosome 8, we identified genes such as *PLEKHA2*, *NBS1*, *NOV* and *MYST3* to be involved in breakpoints. New recurrent alterations were identified on chromosomes 5p, 12p, 13q, 17 and 22 with a common region of acquired uniparental disomy in four samples on chromosome 17q. Single nucleotide polymorphism array results were confirmed by direct sequencing and quantitative real-time polymerase chain reaction.

Conclusions

The first high density single nucleotide polymorphism array allelokaryotyping of T-cell prolymphocytic leukemia genomes added substantial new details about established alterations in this disease and moreover identified numerous new potential target genes in common breakpoints, deletions and regions of acquired uniparental disomy.

Key words: T-cell prolymphocytic leukemia, SNP array, uniparental disomy, copy number change.

Citation: Nowak D, Le Toriellec E, Stern M-H, Kawamata N, Akagi T, Dyer MJ, Hofmann W-K, Ogawa S and Koeffler HP. Molecular allelokaryotyping of T-cell prolymphocytic leukemia cells with high density single nucleotide polymorphism arrays identifies novel common genomic lesions and acquired uniparental disomy. Haematologica 2009; 94:518-527. doi:10.3324/haematol.2008.001347

**These authors contributed equally to the work.*

Funding: we thank the Parker Hughes Fund and National Institutes of Health for grants for supporting this study. DN is supported by a research grant from the Deutsche Forschungsgemeinschaft (DFG, NO 817/1-1), NK is supported by a fellowship from the Tower Cancer Research Foundation. HPK holds the Mark Goodson Chair in Oncology Research at Cedars Sinai Medical Center and is a member of the Jonsson Cancer Center and the Molecular Biology Institute of UCLA. This work was also supported by grant-in-aid from the Department of Health, Welfare and Labor and from MEXT of the Japanese government.

Manuscript received September 30, 2008. Revised version arrived November 17, 2008. Manuscript accepted December 9, 2008.

Correspondence:
Seishi Ogawa, Department of Regeneration Medicine for Hematopoiesis, Graduate School of Medicine, University of Tokyo, 7-3-1 Hongo,Bunkyo-ku, Tokyo 113-8655 Japan. E-mail: sogawa-tky@umin.ac.jp or Daniel Nowak, Division of Hematology and Oncology, Cedars Sinai Medical Center, UCLA School of Medicine, 8700 Beverly Blvd, Los Angeles, CA 90048, USA. E-mail: Daniel.Nowak@cshs.org

The online version of this article contains a supplementary appendix.

Introduction

T-cell prolymphocytic leukemia (T-PLL) is a rare lymphoproliferative disease with a mature T-cell phenotype. The median age at presentation is 63 years.[1] Its clinical course is generally aggressive with a poor response to chemotherapy and median survival times ranging from 5 months to 2 years in patients receiving therapies containing alemtuzumab.[2-5]

T-PLL has several characteristic and recurring molecular lesions. These include an inversion or translocation of chromosome 14: inv(14)(q11q34) or t(14;14)(q11;q32), which lead to juxtaposition of the *T-cell receptor (TCR) α/δ* enhancer regions to the *T-cell leukemia 1 (TCL1)* locus causing deregulated expression of oncogenes located in this region.[4] An alternative translocation associated with T-PLL is the t(X;14)(q28;q11) juxtaposing the *TCR α/δ* to the *MTCP1* gene.[5] Other common molecular abnormalities in T-PLL are deletions on chromosome 11 involving the *ataxia-telangiectasia mutated (ATM)* gene, which has been shown to be mutated in patients with T-PLL, and common chromosomal gains of 8q and losses of 8p.[6-11]

The *TCL1* family of oncogenes enhances proliferation and survival in several lymphocytic malignancies by binding and augmenting activation of *AKT*[12] and inhibiting activation induced cell death via impairment of the *PKCθ* and *ERK* pathways.[13] This is also reflected by the clinical observation of hyperproliferative subsets of T-PLL with high levels of expression *TCL1*.[14] Mutations in the *ATM* gene are known to be the cause of the rare autosomal recessive disorder ataxia-telangiectasia, which is characterized by cerebellar degeneration, immunodeficiency and increased risk of cancer.[15] *ATM* plays a prominent role in the recognition and repair of DNA double strand breaks[16,17] and the frequent disruption of this gene in T-PLL may be an explanation for the genomic instability observed in this disease. The common genomic abnormalities observed on chromosome 8 have not yet yielded any specific target genes, but the breakpoints occurring on chromosome 8 in T-PLL cluster to two regions which contain the *fibroblast growth factor receptor-1 gene (FGFR1)* and the *MOZ* gene, suggesting them as possible candidate genes.[9]

In searches for new T-PLL specific target genes, recent studies have employed techniques such as comparative genomic hybridization (CGH) and 50K single nucleotide polymorphism (SNP) arrays combined with gene expression analysis. These studies have described several differentially regulated genes possibly due to gene dosage effects[18] and *CDKN1B* haploinsufficiency as a new pathogenic mechanism in T-PLL.[19]

Recently, SNP arrays with a higher resolution (250,000 SNPs interrogated per array) have been developed for whole genome mapping.[20] The analysis of genomic DNA with SNP arrays provides two different types of information. One is a data set comprising the intensity data of all SNPs. Since the human genome is diploid, the intensity values are raised to two after normalization, which represents the normal expression of SNPs on somatic chromosomes. A homozygous deletion results in an expression value of zero and a heterozygous deletion in an expression value of one. Amplifications result in expression values of three or higher integer copy numbers. Apart from copy number data, the method also yields a genotype data set which contains the SNP calls of either AA, AB or BB standing for the alleles of the SNPs. This, combined with the copy number data, which allows the detection of acquired uniparental disomy (UPD), which represents allelic imbalance when one allele is deleted and the other one is duplicated or amplified leading to regions with homozygous SNP calls but a copy number of two or higher. These regions typically contain a mutant tumor suppressor gene or oncogene with loss of their normal allele. Use of these high density SNP arrays in combination with a new computational calculation algorithm termed *molecular allelokaryotyping*[21] allows robust and detailed detection of the described alterations without a need for paired normal DNA samples. In the current study, we used this new interrogational power to assess the genomes of 18 T-PLL samples and thereby identify more precisely common submicroscopic genomic lesions and breakpoints and detect novel common genomic lesions and acquired UPD as potential new pathogenic factors in T-PLL.

Design and Methods

Patients and samples

We studied 18 cases of T-PLL (TP followed by the case number). Samples TP-04, -21, -22, -25, -28, -34, -35, -37, -41, -43, -56 and -57 were obtained from the Institut Curie, Centre de Recherche (Paris, France) and are identical to the samples used in the study by Le Toriellec *et al.*[19] Samples TP-651 and -799 came from the Department of Haematology, University Hospitals Leicester (United Kingdom) and samples TP-166, -168, -170 and -172 were from the Department of Hematology and Oncology, School of Medicine, University of Tokyo (Japan). The acquisition and analysis of patients' DNA samples was conducted with the approval of the local ethical committees of the respective institutions.

The diagnosis of T-PLL was established according to the World Health Organization (WHO) classification of hematopoietic and lymphoid tumors. T-PLL genomic DNA was isolated from residual frozen mononuclear cells from leukemic peripheral blood taken at the time of the initial diagnosis. DNA was extracted using a NucleosSpin Tissue kit (Macherey-Nagel, Hoerdt, France). Paired normal DNA was isolated from Epstein-Barr-virus-transformed lymphoblastoid cell lines, which were generated from frozen blood samples of the corresponding patients. All patients had major lymphocytosis. One case (TP56) arose in an individual with ataxia telangiectasia.

High density single nucleotide polymorphism-array analysis

High quality genomic DNA from the 18 T-PLL cases was processed according to the genomic mapping 250K NspI protocol and hybridized to 250K NspI SNP arrays

using the GeneChip Fluidics station 400 and GeneChip scanner 3000 (Affymetrix, Santa Clara, CA, USA) as described previously.[21,22] Data analysis of deletions, amplifications and UPD was carried out using the CNAG software with non-matched references, as previously described.[21,22] Size, position and location of genes were identified with the UCSC Genome Browser *http://genome.ucsc.edu/* and the Ensemble Genome Browser *http://www.ensembl.org/*.

Validation of acquired uniparental disomy and genomic copy number change

For confirmation of genomic copy number changes, quantitative real-time polymerase chain reaction (PCR) was performed on the genomic DNA from the hybridized T-PLL samples and from matched normal DNA from the same patients according to the calculation method described by Weksberg *et al.*[23] Thereby, we confirmed the deletion of the *FOXP1* gene on chromosome 3 in two samples and used a random region on chromosome 2p21 as a reference. Detection of acquired UPD was validated by PCR of genomic DNA and subsequent direct sequencing of SNPs in a region of acquired UPD versus a heterozygous region in sample TP28 on chromosome 17 and compared to direct sequencing of SNPs in the corresponding matched normal sample. All primer sequences are available on request.

Results

Copy number analysis

As expected from previous studies summarizing genomic lesions in T-PLL,[18,24] we found a great abundance of copy number alterations present in the 18 T-PLL samples. In an initial step, we evaluated all losses and gains of genomic material detected by the allelokaryotyping software, which are depicted for each chromosome in Figure 1. We excluded alterations, which were determined to be due to background noise of SNP signals or copy number polymorphisms as recorded in data bases of the UCSC genome browser. The results of this analysis are documented in *Online Supplementary Table S1*. The data re-confirmed characteristic genomic lesions described in T-PLL. Moreover, a variety of other alterations containing interesting putative target genes were detected. In the first systematic measure, we sought to review the above mentioned characteristic lesions on chromosomes 14, 11 and 8.

Chromosome 14

The characteristic inversion inv(14)(q11q34) or translocation t(14;14)(q11;q32) in T-PLL should not be detected by SNP array as no copy number changes occur by these balanced alterations. Interestingly, however, several copy number alterations involving the *TCL* oncogenes were detectable. Sample TP22 displayed a heterozygous deletion in region chr14:95130522-95211348 which partly covers *T-cell leukemia/lymphoma 6 isoform TCL6a3*. Furthermore, five samples had duplications of the telomeric end of chromosome 14 (example, Figure 2A) and a putative breakpoint within the *TCL* oncogenes or in their direct vicinity, distal to them, suggesting that the alterations affecting this site are unbalanced in these samples. The breakpoints leading to duplication or amplification in the respective samples are schematically displayed in Figure 2B, which shows that they lie in typical regions also described for the known translocations.[4] An analysis of the alternate translocation t(X;14)(q28;q11) on chromosome X revealed no unbalanced lesions.

Chromosome 8

The high density genomic mapping carried out in our study revealed broad heterozygous deletions of chromosome 8p in nine samples (50%) and duplications or amplification of chromosome 8q in 13 samples (72%). The detailed mapping of the breakpoints leading to these imbalances revealed that they were scattered over a broad region on chromosome 8p and often displayed highly complex copy number alterations with numerous breakpoints (Figure 2C). In search of genes in the commonly affected regions, we analyzed all chromosomal breaks in all samples on chromosome 8 also including alterations on chromosome 8q. Although an unambiguous common breakpoint could not be identified and most breakpoints were located in regions, that did not

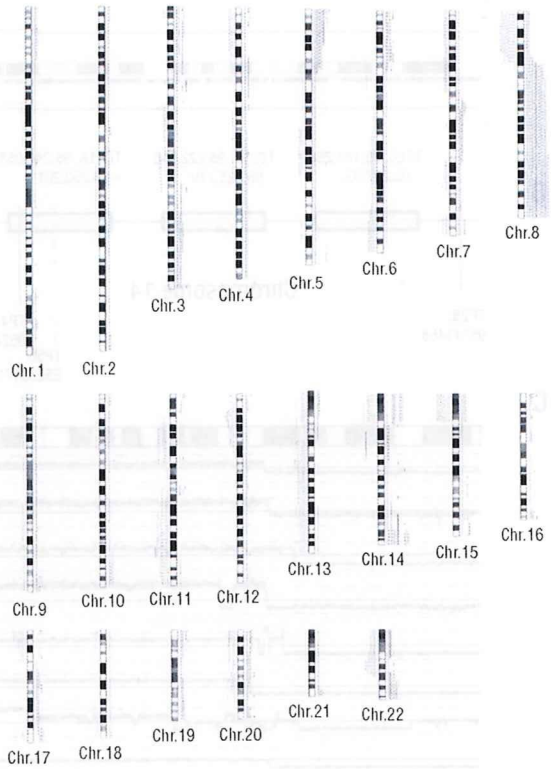

Figure 1. Overview of gains and losses detected by the CNAG software. Lines to the right of the cytobands document gains. Lines to the left of the cytobands represent losses. Each line represents one sample.

contain any genes, some breaks were notable because they were positioned directly within genes and recurred in at least two samples. Breakpoints, that were intragenic are summarized in Table 1. Genes commonly affected by breaks on chromosome 8 were *general transcription factor IIE polypeptide 2* (*GTF2E2*) (two samples), *peroxidasin homolog-like* (*PXDNL*) (two samples), *pleckstrin homology domain containing family A* (*PLEKHA2*) (two samples), *nibrin isoform 2* (NBN) (two samples), *CUB and Sushi multiple domains 3 isoform 2* (CSMD3) (two samples) and *minichromosome maintenance complex component 4* (*MCM4*). Furthermore, in single cases, interesting target genes such as *nephroblastoma overexpressed precursor* (*NOV*) or *MYST histone acetyltransferase monocytic* (*MYST3*) were involved directly in chromosomal breakpoints detected by SNP array.

Chromosome 11

In our study, 12 samples (67%) displayed heterozygous deletions on chromosome 11q, all including the *ATM* gene. Deletions either affected broad regions of chromosome 11q (seven samples) or very discrete deletions specifically targeting the *ATM* locus (five samples). Interestingly, several small defined regions other than the *ATM* deletions were also identified on chromosome 11q.

Sample TP4 displayed a 700 kb heterozygous microdeletion on chromosome 11q33.1 (110891599-111596604), which has its proximal breakpoint in the direct vicinity of two micro RNA, *hsa-mir-34b and hsa-mir 34c*. This micro RNA locus was affected either by chromosomal breakage in the direct vicinity or heterozygous deletion in eight samples (44%). Another region affected by small, confined lesions in several samples contains two members of the *ETS* family of transcription factors, *v-ets erythroblastosis virus E26 oncogene* (*ETS1*) and *Friend leukemia virus integration 1* (*FLI1*). These two genes were contained in heterozygous deletions in seven samples (39%).

Homozygous deletions

Homozygous deletions were abundantly detected on chromosomes 14 and 7 in the T-cell receptor loci. These deletions have to be understood as physiological as part of the T-cell receptor rearrangements and were, there-

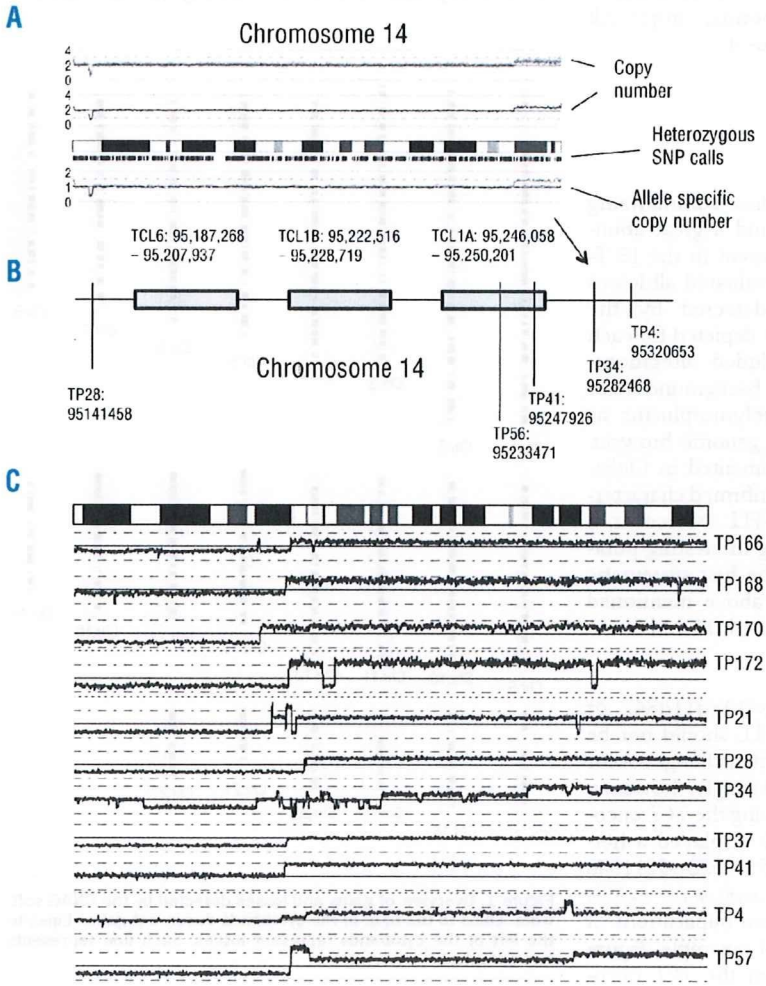

Figure 2. Breakpoints of unbalanced translocations involving the *TCL1* locus and breakpoints on chromosome 8. (A) A view of chromosome 14 in sample TP34 showing a duplication of the chromosomal region 14q32.13 - 14q32.33 harboring a breakpoint in the *TCL1* locus. Similar unbalanced translocations were detected in four other samples, and their breakpoints in relation to the three putative oncogenes *TCL6*, *TCL1B* and *TCL1A* are displayed in the lower panel (B). (C) T-PLL commonly displays a loss of chromosome 8p and gain of 8q. The regions of chromosomal breakpoints leading to this imbalance, as analyzed by high density SNP arrays are displayed. The images show that the breakages are frequently of highly complex nature, containing multiple changes of copy number and breakpoints in individual samples.

fore, excluded from the analysis. Apart from these, scattered homozygous deletions were detected in single samples and are summarized in Table 2. Most of these deletions were single events, not recurring in other samples except for the circumscribed deletion of the transcription factor *forkhead box P1 isoform 1* (*FOXP1*), which was additionally heterozygously deleted in two other samples. Due to this targeted deletion of *FOXP1*, we performed a mutation analysis of this gene by directly sequencing all exons in the samples affected by a deletion. However, this yielded no mutations.

Novel common lesions and acquired uniparental disomy

Besides the common lesions already described, our data showed a cumulation of noteworthy genomic alterations in other loci, which have not yet been described in T-PLL. As shown in Figure 1 and documented in Table 1, the allelokaryotyping software detected ten duplications and amplifications on chromosome 5p. Here, one lesion stood out to be common in three samples (TP172, TP28 and TP56). These three samples displayed a common breakpoint clustering on chromosome 5p within the direct vicinity of the gene *dynein axonemal heavy chain 5* (*DNAH5*). Potentially, this region may represent a common fusion partner to cancer-relevant genes in these samples.

Another hot-spot of alterations was on chromosome 12p, a location long known to be a region for frequent chromosomal rearrangements in hematologic malignancies.[25] Six samples featured heterozygous deletions and four samples had stretches of duplication in this region.

Table 1. Breakpoints involving genes on chromosome 8.

Sample	Breakpoints	Gene symbol / Ref seq (NCBI)	Gene name
TP166	30525448-30556394	*RBPMS (NM_001008711)*	RNA-binding protein with multiple splicing
		GTF2E2 (NM_002095)	**General transcription factor IIE, polypeptide 2**
		ZNF703 (NM_025069.1)	Zinc finger protein 703
TP170	30556573-30567360	*GTF2E2 (NM_002095)*	**General transcription factor IIE, polypeptide 2**
TP172	52424024-52449065	*PXDNL (NM_144651.4)*	**Peroxidasin homolog-like**
	55475848-55486603	*No gene*	
	119646159- 119658006	*SAMD12 (NM_207506.2)*	Sterile α motif domain containing 12 isoform
	120496451- 120498925	*NOV (NM_002514.3)*	Nephroblastoma overexpressed precursor
TP21	32725125-32748740	*NRG1 (NM_013956.2)*	Neuregulin 1 isoform HRG-β1
	38923786-38940822	*PLEKHA2 (NM_021623.1)*	**Pleckstrin homology domain containing family A**
	116672278-116694882	*TRPS1 (NM_014112.2)*	Zinc finger transcription factor TRPS1
TP25	18187886-18309434	*NAT2 (NM_000015.2)*	Arylamide acetylase 2
	90873782-91022515	*NBN (NM_001024688.1)*	**Nibrin isoform 2**
TP34	35377596-35400272	*AY358147 (AY358147)*	Netrin receptor UNC5D precursor
	38784934-38800233	*TACC1 (NM_006283.2)*	Transforming acidic coiled-coil containing
	38901784-38923786	*PLEKHA2 (NM_021623.1)*	**Pleckstrin homology domain containing family A**
	38959748-39003333	*HTRA4 (NM_153692.2)*	HtrA serine peptidase 4
		ADAM9 (NM_003816.2)	ADAM metallopeptidase domain 9 isoform 1
	39992705-40000344	*INDOL1 (NM_194294.2)*	Indoleamine-pyrrole 2 3 dioxygenase-like 1
	41930678-42004277	*MYST3 (NM_006766.3)*	MYST histone acetyltransferase
	48723259-48854459	*KIAA0146 (NM_001080394.1)*	Hypothetical protein LOC23514
		PRKDC (NM_006904.6)	Protein kinase DNA-activated catalytic
	49037364-49184635	*MCM4 (NM_005914.2)*	**Minichromosome maintenance complex component 4**
	51712398-51723458	*SNTG1 (NM_018967.2)*	Syntrophin γ 1
	52578754-52584231	*PXDNL (NM_144651.4)*	Peroxidasin homolog-like
	56339119-56371801	*XKR4 (NM_052898.1)*	XK Kell blood group complex subunit-related
	62477485-62513049	*RLBP1L1 (NM_173519.1)*	Retinaldehyde binding protein 1-like 1
	90991278-91018273	*NBN (NM_001024688.1)*	**Nibrin isoform 2**
	114118249-114142324	*CSMD3 (NM_198124.1)*	**CUB and Sushi multiple domains 3 isoform 2**
	121449563-121485532	*COL14A1 (NM_021110.1)*	Collagen type XIV α 1
		MRPL13 (NM_014078.4)	Mitochondrial ribosomal protein L13
TP4	113993350-114031134	*CSMD3 (NM_198124.1)*	**CUB and Sushi multiple domains 3 isoform 2**
TP57	49037364-49184635	*MCM4 (NM_005914.2)*	**Minichromosome maintenance complex component 4**
		UBE2V2 (NM_003350.2)	Ubiquitin-conjugating enzyme E2 variant 2

A list of all genes that were directly involved in a breakpoint (i.e. a change of copy number) on chromosome 8 in the respective T-PLL samples as detected by molecular allelokaryotyping with 250K SNP arrays. Breakpoint positions are defined by the border SNPs of the detected copy number changes. Sometimes several genes were affected in one sample, as the breakpoints were often complex (see also Figure 3). Genes, that were commonly affected by a breakpoint in more than one sample are shown in bold.